6-10-2014

Molecular and Device Engineering Towards the Study of Potential Anti-MRSA Agents

Powell Fansler
Santa Clara Univeristy

Karla Geisse
Santa Clara Univeristy

Ryan Marshall
Santa Clara Univeristy

Santa Clara University
DEPARTMENT of BIOENGINEERING

Date: June 10, 2014

I HEREBY RECOMMEND THAT THE THESIS PREPARED UNDER MY SUPERVISION BY

Ryan Marshall, Karla Geisse, and Powell Fansler

ENTITLED

Molecular and Device Engineering Towards the Study of Potential Anti-MRSA Agents

BE ACCEPTED IN PARTIAL FULFILLMENT OF THE REQUIREMENTS FOR THE

DEGREE OF

BACHELOR OF SCIENCE IN BIOENGINEERING

Zhiwen Zhang

THESIS ADVISOR

DEPARTMENT CHAIR

MOLECULAR AND DEVICE ENGINEERING TOWARDS THE STUDY OF POTENTIAL ANTI-MRSA AGENTS

by

Ryan Marshall, Karla Geisse, and Powell Fansler

SENIOR DESIGN PROJECT REPORT

Submitted in partial fulfillment of the requirements
for the degree of
Bachelor of Science in Bioengineering
School of Engineering
Santa Clara University

Santa Clara, California

June 10, 2014

Abstract

At the intersection of bio-device engineering and bio-pharmaceutical studies, our project involved the design of a hydraulic manifold to be used in isothermal titration calorimetry (ITC), with the ultimate goal of using ITC to study the thermodynamic binding parameters of potential anti-Methicillin Resistant *Staphylococcus aureus* (MRSA) agents to our drug target, Sortase A. The hydraulic manifold redesign included the analysis of materials such as high density polyethylene (HDPE), polytetrafluorethylene (PTFE, 'Teflon'), and polycarbonate as well as the implementation of a new construct of the manifold itself. Sortase A is a transpeptidase found in Gram-positive bacteria and catalyses the attachment of virulent surface proteins to the cell wall by recognizing a specific amino acid motif (LPXTG). The ability of the bacterium to communicate with and infect host cells is linked to the Sortase A mechanism. We have identified pyridostigmine bromide as the primary drug target based upon the analysis of ITC data.

Acknowledgements

We would like to recognize Professor Zhiwen Jonathan Zhang for his mentorship throughout this entire project.

We thank the School of Engineering for their generous financial support of this project.

We'd like to acknowledge Olaotan Elenitoba-Johnson, who was instrumental in assisting us with troubleshooting the issue with the ITC and re-designing of the hydraulic manifold.

Additionally, this project would not have been possible without the generosity of Professor Daryl Eggers at San Jose State University, who allowed us space in his laboratory to carry out experiments using his MicroCal VP-ITC.

Table of Contents

List of Abbreviations

ITC - Isothermal Titration Calorimetry

SrtA - Sortase A

PB - Pyridostigmine Bromide

MRSA - Methicillin-resistant *Staphylococcus aureus*

HDPE - High-density polyethylene

PTFE - Polytetrafluoroethylene ('Teflon')

S. aureus - *Staphylococcus aureus*

LB - Luria Broth

E. Coli - *Escherichia coli*

IPTG - isopropyl β-D-1-thiogalactopyranoside

GE- General Electric

List of Figures

List of Tables

Introduction and Significance

Background & Motivation

Staphylococcus aureus (*S. aureus*) is a species of bacteria capable of multidrug resistance, and is the causative agent of a multitude of ailments such as meningitis, skin infections, and food poisoning. The most concerning strain of antibiotic-resistant *S. aureus* from a public health standpoint is methicillin-resistant *Staphylococcus aureus* (MRSA). This is because resistance to methicillin confers resistance to all penicillinase-resistant penicillins and cephalosporins. These are considered broad-spectrum antibiotics, which is what makes MRSA infections so challenging to treat. In addition, there has been an increasing number of reports of vancomycin-resistant strains, which suggests that full resistance to vancomycin may eventually emerge as well [1].

The incidence of community-acquired and hospital-acquired MRSA infections has increased rapidly over the past decade. In the Active Bacterial Core Surveillance database (which covers nine geographic regions and represents 4.4 million children under the age of 18), it was shown that community-acquired MRSA cases have particularly increased in African-American children and in infants younger than 90 days [2].

Antibiotic resistance is a phenomenon that arises through the process of evolution, and it can be accelerated by continually exposing bacteria to antibacterial drugs. Traits that make a bacterium resistant to antibiotics are replicated during cell division, and are passed on from generation to generation. Antibiotic resistance reduces the effectiveness of certain treatments, keeping patients in the hospital for longer and increasing the risk of spreading antibiotic-resistant bacteria. The World Health Organization (WHO) has claimed that the emergence of these new antibiotic resistance mechanisms will render the latest generation of antibiotics virtually ineffective within the next 20-30 years [3].

As such, it would be of immense benefit to develop a new type of antibiotic that does not function in the same fashion as current and former antibiotics. What our project sets out to do is to identify an inhibitor of Sortase A (SrtA), a transpeptidase found in *S. aureus*

that acts in the translocation and sorting of proteins to the cell surface. Inhibition of SrtA would prevent the attachment of certain proteins to the bacterial surface. Many of these surface proteins play key roles in pathogenic mechanisms of the bacteria: invasion of host cells, adhesion to host cells, and evasion of the host immune response. Surface proteins can also play a role in cell division, cell wall maintenance, and the acquisition of nutrients from the environment. However, by the very nature of its role in the cell, SrtA is not an essential protein for the survival of the bacteria. Thus, inhibition of SrtA will not induce the same selective pressure that current antibiotics do because bacteria that are resistant to SrtA inhibition will not be selected for [4].

Review of Literature

Our project involved employing Isothermal Titration Calorimetry (ITC) to study and quantify the binding of small molecules to SrtA. Our literature review provided no evidence of the use of SrtA as a drug target in an ITC experiment. However, SrtA has been studied as a drug target through alternative methods, while ITC has long been extensively used as a tool in drug discovery. Thus, our literature research was focused on the applications of ITC in the field of drug discovery, as well as existing models of SrtA inhibition. Our review of literature with respect to ITC encompasses experimental design and data analysis, techniques in studies involving systems with low binding affinity, and previous experiments for which ITC has been used to elucidate binding of small molecules to proteins. We also looked carefully into SrtA, its structure and mechanism, its dimerization properties and characteristics, and important interactions with common cations. In addition, we looked into previously determined SrtA inhibitors to review existing methods and technologies.

ITC Experimental Design and Data Analysis

Our literature review of ITC experimental design provided us with insights on planning experiments. This involved determining the starting concentrations of both the drug candidate and SrtA, such that the heat released upon each injection is sufficient to yield quantifiable binding parameters [5]. In addition, proper handling and preparation of solutions has been demonstrated to be of vital importance to the integrity of ITC

experiments. To reduce artifact heats as much as possible, it is recommended to use filtration and dialysis, as well as matching the solutions on criteria such as pH, buffer, and salt concentration [5].

Literature on ITC data analysis stresses the importance of using control experiments. Simple blank corrections can be made to the data by subtracting out data collected from control experiments [5]. Once ITC data has been corrected for any artifact heats, the ITC software can fit the data using nonlinear regression models. In order to do this, a binding model must be assumed; we must make predictions about the nature of the binding being observed [5]. These non-linear regression models are what provide us with the binding stoichiometry, association constants, enthalpy values, and entropy values that characterize the binding event.

Relevant ITC Uses

One of the identified constraints of our project was the likely event that binding between certain drug candidates and SrtA will be weak. Traditionally, weak binding events require ITC users to increase the concentration of the ligand (in our case, the drug candidate) in order to achieve measurable thermodynamics. However, users soon run into a problem when the concentration required to achieve observable and reliable data exceeds the maximum concentration at which the ligand is soluble in the chosen buffer. This fact renders the ITC virtually ineffective for some drug candidates, unless proper action is taken, as we found in our literature review. The most common technique is to freeze the binding stoichiometry parameter when fitting the data. It has been shown that estimates of the binding constant parameter obtained by freezing the binding stoichiometry parameter are “virtually independent” of any error in binding stoichiometry for systems with weak binding [6].

Researching previously determined binding parameters of small molecules to proteins gave us insight into the nature of protein-small molecule interaction. For example, the binding of statins to HMG-CoA reductase demonstrates the effective use of the solvent DMSO, as well as the careful consideration of ionization enthalpies of selected buffers

[7]. Further literature review of example experiments confirmed the importance of solution pH matching, filtration, experimental design, and the use of controls.

Properties of SrtA

From our literature research on SrtA, we had collected valuable information regarding its structure [8], properties such as dimerization [9] and calcium ion binding [10], as well as its mechanism of action [8,10]. This aspect of the literature allowed us to understand and interpret the reactions inside the ITC on a more fundamental level. It also affected our experimental design; for example, calcium has been shown to increase the activity of SrtA eight-fold at a concentration of just 2mM [10]. In our experiments, SrtA was incubated with 2mM calcium chloride in order to ensure maximum enzymatic activity.

Known SrtA Inhibitors

Heavily researched inhibitors include: vinyl sulfones [11], isoquinoline alkaloids [12], and some medicinal plants [13]. The inhibitory activity of each of these compounds was determined using fluorescence readings. SrtA was incubated with a peptide containing its substrate sequence flanked with a fluorophore and a quencher. An active SrtA cleaves the peptide, separating the fluorophore from the quencher and yielding fluorescence. Inhibition is thus detected via the decrease in fluorescence compared with the absence of an inhibitor.

ITC Washing Module Hydraulic Manifold

Due to the sole proprietor of the ITC washing module's hydraulic manifold being GE Healthcare, the knowledge of any previous design and reasons for such design are unknown to the general public. For information regarding the reasons for the selection of the prototyping material see Chapter 2.

Evaluation of Current Technologies

ITC is widely used as a tool in drug discovery because of its high sensitivity and its ability to directly and simultaneously measure all thermodynamic binding parameters in a single experiment [14]. However, some experimenters choose not to use ITC due to some

of its inherent constraints. As described above, some users find ITC unsuitable for use in characterizing the binding parameters for weak binding pairs, while still others find the instrument is limited by its sample consumption and the time required to perform an experiment [14].

However, given the stage of our drug candidates, we found the ITC a suitable and highly effective technology. Other methods involved the measurement of enzyme activity, as described above. This method is effective in identifying inhibition, but it does not yield stoichiometric or thermodynamic data that the ITC will (see Results). Thus, ITC provides a clearer picture of the binding event of the inhibitor to the protein. The enzyme kinetics approach also requires labeling, and the use of an indirect measurement, such as fluorescence. ITC is unique in this way in its ability to directly measure thermodynamic binding using a label-free, in-solution technology that does not require either of the targets to be surface-immobilized [14].

Project Goals

Diagnose the Issues with the MicroCal iTC200

For a string of months prior to beginning our project, the MicroCal iTC200 housed within Santa Clara University's Bannan Engineering Labs was left idle. The instrument functions at its best when it is operated relatively consistently. When we first set out to use the ITC it did not produce reliable background data, thus, a thorough analysis of the fault and a correct diagnosis for complete restoration was necessary in order to obtain significant data.

Design and Test Hydraulic Manifold Prototypes

As the diagnosis was completed, we identified the issue with the ITC washing module to be the manifold. We tested multiple manifold prototypes of our own design to increase the overall efficiency of the instrument.

Solubilize Compounds

The medium for experimentation must be aqueous in order to preserve SrtA's enzymatic functionality. The sensitivity of the ITC required that our solutions be entirely homogenous, otherwise inaccurate thermodynamic readings would be obtained. Depending on how soluble each compound was in our chosen aqueous buffer, varying amounts of cosolvent were necessary to add to facilitate dissolution. If cosolvents were required, additional testing on their impact on protein stability and activity was completed

Protein Purification

In order to assess the binding affinity between SrtA and the drug candidates, we must be able to consistently produce a pure and active protein. We carried out a well-established protein purification protocol to express, isolate, and purify the proteins from *Escherichia coli*.

Isothermal Titration Calorimeter Testing

The ITC acquires data by comparing the Reference Cell's and the Sample Cell's thermodynamic data. Thus, if a molecule is able to bind to SrtA, the instrument will be able to pick up the thermodynamic signal produced by the binding activity, which then in turn can be interpreted via ORIGIN software to elucidate both thermodynamic and kinetic data on the reaction.

Further Testing for Publishable Data

In order to obtain significant data, reproducibility of the experiment is the foremost objective. Thus, each compound was tested in repetition in order to ensure the accuracy of the results.

Expected Results

We were examining the compounds in order to obtain a significantly strong binding to the SrtA protein; thus, ideally, at least one of the compounds would have a binding similar to the ideal thermodynamic data presented below (Figure 1).

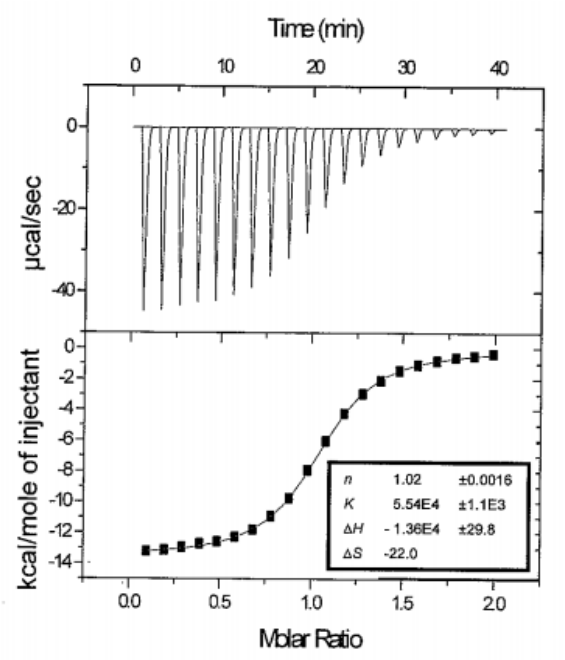

Figure 1. Ideal ITC data. The graph at the top displays the raw data of the titration. The graph at the bottom displays the integrated data points, generated by the ORIGIN software. Titration of Calcium into EDTA Taken from MicroCal^{TM}iTC$_{200}$ system User Manual.

Ideal ITC Data Characteristics to Emulate

1. Low amount of error (seen in the small ± values)
2. Smooth sigmoidal curve in order to calculate the stoichiometry (n) and the affinity (K) (Figure 2)

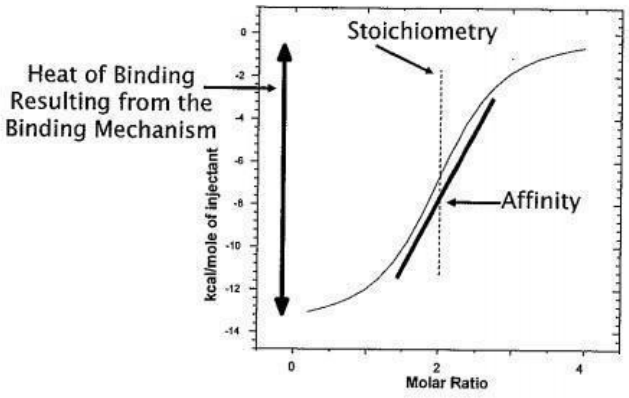

Figure 2. Method of determination of various binding parameters. Provided by the MicroCal^{TM}iTC$_{200}$ system User Manual.

MicroCal iTC200 Expected Results

Once the issue with the MicroCal iTC200 had been identified and replaced/repaired, there should be uniform fluid flow throughout the washing module. Thus, the instrument should be capable of cleaning the reaction cell to ensure accurate data acquisition.

Back Up Plans Regarding Objectives

Repairing the ITC

It is of utmost importance that the instrument was repaired; our experimentation depends entirely on the functionality of the device. Thus, in this particular case, if the instrument did not obtain functionality, if possible we would lease a similar instrument from an outside source for experimentation. A more in depth description of this issue is seen in Chapter 1.

Solubility

If an individual compound studied was determined to be insoluble, varying amounts of cosolvents were added to facilitate dissolution. If cosolvents were required, additional testing on their impact on protein stability and activity was necessary. Some compounds required more cosolvent aid than will be safe for protein activity - these proved to be the toughest to experiment on. A successful ITC experiment relies on appropriate and thorough controls. The inclusion of cosolvents required additional control experiments such that any heats generated by the presence of the cosolvent can be subtracted from the experimental data. In general, the more elements in solution during an ITC experiment, the more complicated and precise controls are necessary in order to cross-check the potential for heat generation between any two solutes.

Protein Purification

Issues with the purification protocol would most likely stem from some sort of contamination, in which case we would reexamine the sterility of our techniques and proceed from there. However, the likelihood of an issue arising from this particular stem

in our experiment was unlikely as the procedures are quite well established, and SrtA is not a difficult protein to isolate and purify.

Isothermal Titration Calorimeter Testing

Example of abnormal thermodynamic data (Figure 3).

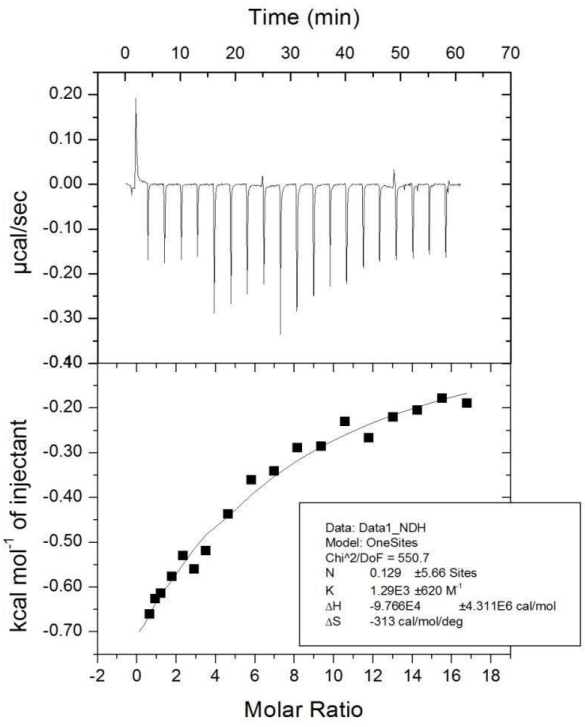

Figure 3.Non-Ideal Isothermal Titration data. First graph is the raw thermodynamic data. Second graph is ORIGIN® software analyzed data. Titration of Calcium into SrtA.

ITC Data Characteristics to Avoid

1. Abnormal vertical peaks (seen in the above graph) above the baseline
    i. These indicate air bubbles that hinder the data analysis software, ORIGIN, calculations
2. Extremely large error values
    i. The error values above indicate that this data is not significant.
3. Irregular patterns of thermodynamic data
    i. In order for the ORIGIN software to be most effective, the sigmoidal curve or similar is the most optimal

Process of Correction for Irregular Data

1. Repeat test to ensure that testing parameters need to be changed.
2. Change testing parameters on the ORIGIN software
    i. Change titration volumes or number of titrations
    ii. Change experimental temperature
3. Assuming there was no extraneous thermodynamic data when completing the controls, the issue must be with the machine itself; check the ITC with the standards provided in the set-up kit to ensure functionality

Significance

Drug Target Analysis

The goal of our project was to elucidate and quantify the binding of small molecules to SrtA, a transpeptidase found in Gram-positive bacteria such as *S. aureus*. SrtA was a rational drug target because its inhibition results in the loss of pathogenicity in that bacterium. What is doubly advantageous about targeting drugs to inhibit SrtA is that successful binding candidates will not be lethal to the bacteria because the action of SrtA is not essential to the bacterial fitness. This releases the pressure for evolution, and in this sense, small molecules that bind to SrtA will not be antibiotics, they will be anti-infectives.

High-throughput screening of compounds was completed in house to determine the inhibition of Sortase A *in vivo*. We tested their binding capabilities to the SrtA enzyme *in vitro* to determine which, if any, strongly bind to the enzyme. If one of the twenty-one shows strong enough binding for SrtA *in vitro*, it could be considered a potential drug candidate with the possibility of going through the steps necessary for Food and Drug Administration approval. We targeted pyridostigmine bromide as the compound having the most potential due to its chemical structure (further explained in Chapter 3).

The impact of an anti-infective will have a longer duration of use as a result of the minimal evolutionary pressure; as such, it will be contain a longer duration of effective

use. It will be more difficult for the bacteria to gain resistance to the anti-infective as the native population of a bacterial culture will not undergo the selective measures induced by the implementation of antibiotics.

There will also be a need for the anti-infectives as the antibiotics will no longer be capable in their attempt to suppress infections. As said above, antibiotics are becoming less and less effective, eventually they will lose their applicability entirely. As such, a replacement in the treatment of these types of diseases will be necessary for the healthcare field in general.

Hydraulic Manifold Design

Once the hydraulic manifold was designed with optimized characteristics for functionality, this component would be able to repair our in house MicroCal iTC200. We would then be able to complete experimentation much more efficiently as we would not have to relocate to acquire the data.

The designed manifold will also be of use to General Electric's Life Sciences department (the manufacturer or the MicroCal iTC200) if they incorporate the design into a later model of the instrument. Our design process incorporated materials that would lessen the cost of the device while increasing its operable timespan.

Team and Management

Table 1. Responsibilities of all supporting members of our design project.

Team Members	**Responsibilities**
Karla Geisse Ryan Marshall Powell Fansler	Srt A purification, solubilization of drug candidates, ITC experimentation, hydraulic manifold design
Professor Zhiwen Zhang	Project oversight, management of laboratory funds
Professor Daryl Eggers	MicroCal VP-ITC training and assistance
Olaotan Elenitoba-Johnson	MicroCal ITC200 diagnosis assistance, hydraulic manifold design assistance
Blake Williams Elyse Shimomura	Autoclave materials, general laboratory assistance as graduate students with more experience in this field

Timeline

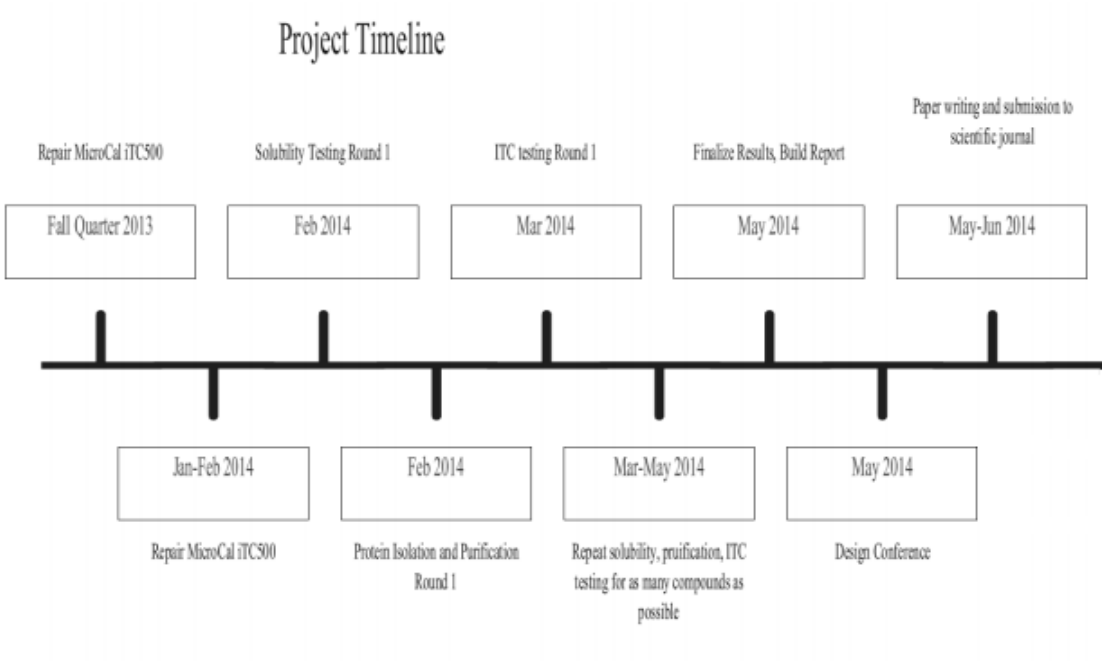

Figure 4. Timeline. Initial timeline for progress of experimentation

Budget

Table 2. Budget for Compounds being tested.

Compound Budget			
Compound	**Source**	**Mass (Milligrams)**	**Price (Dollars)**
Alpha Lipoic Acid	Sigma Aldrich	500	15.00
Atracurium Besylate	LKT Laboratories, Inc.	50	56.40
6-Hydroxydopamine Hydrochloride	Sigma Aldrich	100	95.60
Synephrine	LKT Laboratories, Inc.	1000	30.00
Pyridostigmine Bromide (Mestinon)	Sigma Aldrich	1000	91.60
(R)-(-)-Apomorphine Hydrochloride	Sigma Aldrich	100	40.60
Risedronate Sodium	Sigma Aldrich	50	89.00
Granisetron Hydrochloride	Tocrisis Bioscience	10	65.00
Coenzyme B12	Sigma Aldrich	25	43.80
Total Cost of Compounds	$ 527		
Estimate Re-orders	3		
Cost Per Quarter	$ 527		
Estimate Net Cost for the Year	$ 1581		

Table 3. Budget for Protein Purification

Protein Purification Budget			
Item	**Source**	**Mass**	**Price (Dollars)**
HEPES buffer	Sigma Aldrich	25g/100g	35.80/46.60
Protein Purification General Laboratory Materials*	varies	varies	varies
Cost per Quarter	varies		
Estimate Net Cost for the Year	varies		

* will depend on other students' use of similar materials in the same laboratory

Chapter 1: Compromised Manifold

Introduction

This chapter discusses the complications that we encountered with the ITC's washing module. The washing module's purpose is to clean the injection syringe, sample cell, and reference cell of the ITC; without the ability to thoroughly clean these components, the thermodynamic measurements would be rendered insignificant due to extraneous heat included in data acquisition. In addition, due to the constraints of our budget and the privacy of the specifications for the washing module from the manufacturer, our efforts to debug and fix the unit were conducted almost entirely blind, except for basic generalities provided by General Electric (GE) Healthcare Life Sciences technical service.

Through email and phone conversations with GE Healthcare's technical service the parts of the washing module to investigate, which are the most likely candidates for rendering the unit dysfunctional, were obtained (Table 4). Due to the level of privacy that GE Healthcare has for the ITC, there are no forums or engineering drawings available for the washing module that would shed light on how the unit is designed and constructed. Actions taken outside of the scope that GE Healthcare suggested are listed in Table 5 which, when combined with Table 4, illustrates the thorough investigation of the washing module's components. In the next section, the constraints that are listed in Table 4 and Table 5 are discussed and analyzed in order to demonstrate the effect each complication would have on fluid flow.

Table 4. Courses of action recommended by GE Healthcare.

PART	RECOMMENDED ACTION
Connection tubes	Replace
Fill port adapter	Check if clogged (clean with wire, run water through)
Cell cleaning device	Check if clogged
Injection syringe	Check if clogged (pass water through, analyze flow)
Internal filter	Replace

Table 5. Actions performed after completing the suggested actions provided by GE Healthcare

PART	PERFORMED ACTION
Buffer, water, and methanol filter	Checked for clogs
ITC Origin software	Checked for communication issues between the computer and washing module
Washing module microchip	Checked for loose or broken connections Checked if operating correctly
Internal pump	Checked pump for suction strength Realigned flapper valve in correct orientation Compared with internal push pump
Buffer, water, methanol, and waste faceplate	Checked for clogs Checked for leaks
Washing module manifold	Checked for leaks Checked for clogs in microchannels Checked if microchannels are compromised
Master solenoid	Checked for actuation Checked if directed fluid flow correctly
Support solenoids	Checked for actuation Checked if directed fluid flow correctly

Details of Key Constraints

In order to discuss the effects that each component of the washing module would have on the generation and mediation of fluid flow, knowledge of the purpose of the washing module is imperative. To complete a measurement of a molecular interaction, the protein in its matrix is manually added to the sample cell. The addition of the inhibitor to the reaction cell occurs via the loading syringe; the uptake and dispel of the sample is controlled by the washing module. The C1 and C2 ports of the washing module are responsible for the loading of liquid and dispelling of waste that enable the loading of sample into the sample cell, as well as the cleaning of the reaction and reference cell and injection syringe. It is imperative that the C1 and C2 ports are able to deliver and expel liquid so that the measurements made by the ITC do not involve any thermodynamic additions given off by contaminants in the reaction cell.

The connection tubes (Table 4) are the bridge between the buffer, water, methanol, and waste containers to the washing module, as well as the link between the washing module

and both the cell cleaning device and loading syringe. If any of the connection tubes are clogged, the flow through the tube(s) would be inhibited and result in a cease of fluid flow or a dramatic dampening effect. The filter attached to the connection tubes (Table 5) also has a substantial impact on the distribution of liquid through the entire system. If one of the filters attached to the connection tube(s) is clogged, the uptake of water, methanol, and buffer would be impeded, and no liquid would flow through the washing module, and thus, never enter the injection syringe or sample and reference cell.

The internal filter (Table 4) is responsible for preventing any contaminants from traveling into the internal suction pump. A clogged internal filter would increase the difficulty of airflow through the internal film of the filter and result in a decreased efficacy of the suction pump's ability to uptake fluid. When the internal suction pump cannot provide the amount of force needed to carry water, buffer, and methanol to the washing module, no fluid would travel into the injection syringe or to either the sample or reference cell. The flapper valve of the suction pump would also inhibit the force of the pump and result in no fluid flow if the orientation of the valve is incorrect. The flapper valve allows for air to flow in a particular direction by closing off the path to air when the pump is operating. If the orientation of the flapper valve is incorrect, then the correct path that needs to be blocked to the incoming air would be open and the suction would be inhibited. Due to an increase in the amount of channels that air can flow into the pump, the velocity of air inflow would decrease, consequently decreasing the amount of suction provided by the internal pump.

The fill port adapter and cleaning device (Table 4) are the key components that allow for the injection syringe and sample and reference cell to be filled and cleaned. A clog in the fill port adapter would impede inflow to the injection syringe, resulting in no fluid entering the washing module because of the back pressure created by the clog. With no fluid entering the injection syringe, the expulsion of waste would prove to be nonexistent because there is no fluid to be dispelled. Alternately, if the injection syringe has a clog the impedance of fluid flow that would result from a clogged fill port adapter would also be observed. If the fill port adapter was removed and it was seen that liquid had passed

through it (fluid flow was normal) the assumption that the fill port adapter would not be clogged would be correct. Although in the event where there is no fluid flow that is observed, the assumption that the injection syringe was clogged is appropriate. In addition, a clog in the cleaning device would inhibit the flow into the sample and reference cells, resulting in no fluid flow into / out of both cell chambers towards/away from the washing module.

The buffer, water, methanol, and waste faceplate and washing module manifold (Table 5) can also prove to interfere with fluid flow if compromised. The buffer, water, methanol, and waste faceplate serve as the connection to the ends of the buffer, water, methanol, and waste connection tubes. A clog in the face plate would inhibit the ability for liquid to pass through the channels in the face plate for the desired liquid. Suction would also be inhibited because air flow through the desired channels would be dampened. A clog in the washing module manifold would impede liquid flow through the microchannels and result in no fluid passing through the entire system. The microchannels can also be corroded, if the liquid being passed through the channels is left dormant for a substantial amount of time. If a microchannel in the manifold has a leak, liquid separation would be compromised and suction and/or pumping of fluid would be inhibited as the area of liquid flow had been increased. Therefore, if there is a clog in the face plate or manifold or if the manifold has been corroded, no fluid would be observed flowing through the entire system.

The master and supporting solenoids (Table 5) are responsible for directing the type and direction of liquid flow. The master solenoid is responsible for opening the valve that allows for water, buffer, or methanol inflow as well as waste outflow. The supporting solenoids act secondary to the master solenoid by directing the desired fluid to flow in the desired direction once the master solenoid opens and allows for influx of specific liquid. If the master solenoid is not actuating properly and the valve is left open or closed, this would only allow for one specific liquid to flow (if the master is open) or result in no liquid flow (if the master is closed). Additionally, if the supporting solenoids are not actuating properly and remain open/closed, this would have the same impact as the

master solenoid not actuating properly as one specific fluid would have the ability to flow or all fluids would be inhibited.

An aspect of the washing module which could result in no flow of fluid is the section of the unit responsible for directing the actions of the system: the ITC analysis software ORIGIN and the washing module's microchip (Table 5). ORIGIN is the interactive software that allows the user to perform the washing and loading tasks in order to clean the sample and reference cell, loading syringe, and load the sample into the loading syringe. In order for ORIGIN to operate correctly, the washing module's microchip must be functional in order for the software and the device to communicate and operate correctly. If the microchip has a wire disconnected or liquid leaked onto the chip while the unit was operating, it is possible for a short in the systems circuit to occur and communication between ORIGIN and the washing module to be inhibited. Without proper communication between the analysis software and the washing module, any cleaning or loading tasks would be thwarted and fluid would cease to flow.

Design Description

In order to find a solution to the inhibition of the washing module's fluid flow, each section of the washing module was investigated in a systematic and logical order. After gaining insight on the most common problems that arise within the unit (Table 4), provided by GE Healthcare's technical service, we investigated the items that GE Healthcare suggested. In order to ensure the connection tubes were not clogged, we replaced all tubing and end connections. After the connection tubing was replaced, the next part of the washing module to analyze was the fill port adapter. In order to test the adapter for clogs, a fill port syringe was utilized in order to push deionized water through the adapter and a cleaning wire was passed through the channel of the fill port adapter. Once the fill port adapter was checked for clogs, the cell cleaning tool was also checked for clogs with the cleaning wire. When both parts were determined to lack clogs, the loading syringe was analyzed for malfunctions. Connecting the fill port adapter to the loading syringe and manually pushing water through the syringe, we were able to analyze

the inflow and outflow of the deionized water. The loading syringe was determined not to be the cause of the instrument's lack of functionality.

After exhausting the external options that GE Healthcare recommended (Table 4), an inspection of the washing module's internal filter was performed. The washing module's external case was removed and the all wires (power, USB, ground) were removed in order to expose a clear space to reach the internal filter. The internal filter was then replaced to determine if the issue was a clog in that particular part of the device. There was no seen effect after changing the filter.

Following the investigation of the suggested parts of the washing module, a more thorough inspection of the rest of the external and internal parts was performed (Table 5). The last external parts of the washing module to inspect were the buffer, water, and methanol filters to distinguish if there was a clog within the filters. In order to test if there was a clog within the filters, the connection tubes were removed from the washing module and only connected to the containers of liquid. The containers were held upside down to determine if gravity presented enough force for the liquid to flow through the filters and out of the tubes. Once the buffer, water, and methanol filters were determined to be unclogged the inspection of the internal pieces of the washing module were analyzed.

The first of the internal components to be analyzed was the washing module's microchip and the communication between the unit and the analysis software ORIGIN. The microchip has a built in Light Emitting Diode (LED) light that gives off green light when working properly and red light when dysfunctional. The ORIGIN software tests the unit for functionality upon start up; we ran the module and it was seen to be functional. If ORIGIN and the washing module were not communicating properly, the software would not start correctly and prompt the user to fulfill a diagnostic task (check power connections, USB connections). When the microchip and ORIGIN software were checked and were found to be operational, we investigated further into the internal portion of the washing module.

The washing module's internal pump, buffer, water, methanol, and waste faceplate, washing module manifold, and master and support solenoids were the last of the internal components to be analyzed. First, the internal suction pump was analyzed to see if the flapper valve had the correct orientation and that the force of the suction was comparable to the force of the internal push pump. In order to analyze the flapper valve, four screws were removed from the suction pump's case which exposed the flapper valve. After checking for correct orientation, the flapper valve was placed inside the case and the external case was put together. To compare the suction force to the blow force that the air push pump provides, the internal filter was removed from the suction pump and the push pump was removed from its connection tube and each force was compared manually.

The buffer, water, methanol, and waste faceplate and the washing module manifold were tested for clogs via warm water sonication at 42^{o}C for an hour. After the sonication, any clogs or contaminants were removed from within the microchannels. In order to determine if the master and supporting solenoid(s) were actuating properly, we collaborated with Olaotan Elenitoba-Johnson, a Chemistry laboratory technician at Santa Clara University, and he performed diagnostics via vibration detection.

Supporting Analysis and Expected Results

After performing the diagnostics on each part of the washing module in Tables 4 and 5, both a cell and loading syringe cleaning test were performed in order to determine if liquid flow had been fixed. When the connection tubes and internal filter were replaced, flow impedance persisted. In addition, after cleaning the fill port adapter and cell cleaning tool with the cleaning wire and passing deionized water through each, fluid flow continued to be inhibited. The impedance of flow after replacing and cleaning the connection tubes, internal filter, fill port adapter, cell cleaning tool, and injection syringe illustrated that the washing module's fluid flow problem was either with communication between the computer and the unit or the water, buffer, or methanol filters were completely clogged.

When running the ORIGIN software, it detected no communication problems with the washing module and the module's microchip consistently had a flashing green LED light. This allowed us to reason that there were no connection problems within the washing module as far as the microchip was concerned. The filters of the water, buffer, and methanol containers were then tested for clogs. After holding all containers upside down and disconnecting the tubes from the face of the washing module, liquid was able to flow out of the tubes. Due to the ability of liquid to flow through the connection tubes, the filters within the containers were not clogged, which meant that the issue with the washing module was completely internal.

The investigation of the internal suction pump proved to be successful in that the orientation of the flapper valve was off-set and in effect decreasing the amount of suction. Orienting the flapper valve correctly and comparing the suction strength to the blowing force that the air pushing pump provided, the forces were comparable in magnitude. After increasing the amount of suction provided by orienting the flapper valve correctly, we performed a cell and loading syringe cleaning test to check if flow inhibition has been solved. Although immediately following the initialization of the test, the fluid flow remained inhibited

The analysis of the buffer, water, methanol, and waste faceplate and washing module manifold was conducted following the internal suction pump. After water sonicating both parts for an hour in 42^{o}C, there proved to be no contaminants or debris in the water afterwards. Following sonication, the washing module was assembled and the cell and loading syringe cleaning tests were performed; impedance of fluid flow persisted.

The last part of the washing module to inspect was the master and supporting solenoids. The vibration analysis was performed by Olaotan Elenitoba-Johnson and the results were uncertain. Due to the solenoids having cemented manifolds, visual actuation detection could not be performed. After the vibration analysis, a final cell and loading syringe cleaning test was run and presented with the same result: inhibition of fluid flow.

Due to the persistence of fluid inhibition after analyzing all components of the washing module, we ordered a new master solenoid and support solenoids in hope that this would solve the washing module's fluid flow impedance. With new solenoids, the valves of the washing modules manifold would be properly opening and closing and would illustrate if the issue was a continually closed or open valve.

Back-Up Plan

In the event that the master solenoid and supporting solenoids were ordered and properly installed and the washing module continued to have fluid flow impedance, we would attempt to lease an ITC through a laboratory company or perform our research at a research institution with the required lab equipment. If we were unable to find an ITC to lease or a laboratory to perform our research, the analysis of our inhibitor candidates with SrtA could be performed through enzyme kinetic assays.

Materials & Methods

In order to replace the connection tubes of the washing module the extra polyurethane tubing provided by GE Healthcare was utilized. Both ends of the broken tubing were unscrewed and the new tubing was screwed in its place. To replace the internal filter, internal filters were ordered from GE Healthcare through their technical service department. Once the internal filters arrived, the washing module was disassembled and the old internal filter was unscrewed and replaced with the new filter. To check for clogs amongst the buffer, water, and methanol filters, as well as the buffer, water, methanol, and waste faceplate deionized water was passed through the filters and faceplate ports in order to dislodge any clog and to detect if there was a clog. To diagnose the fill port adapter and cell cleaning tool for any clogs the cleaning wire (provided by GE Healthcare) was passed through both pieces and deionized water was additionally pushed through.

To determine if the ITC Origin software was communicating correctly with the washing module the USB connection port was analyzed for a true connection. In addition to checking the USB connection port between the computer and the washing module, the

Origin software has a built in analysis program that verifies communication between the two systems before successfully booting. Therefore when the software booted correctly the Origin software visually illustrated that correct communication between the washing module and the computer was achieved. To diagnose the washing module microchip, the LED light which flashes green when the microchip is behaving correctly and red when it is dysfunctional was inspected. In order to verify that the solenoids (master and support solenoids) were actuating correctly and directing fluid flow properly, audible vibrational analysis was performed with a small steel rod.

Results

After analysis of every component (except for the hydraulic manifold) of the washing module, the system continued to have an impedance of fluid flow. The diagnosis of all components in Tables 4 and 5 were negative proving that none of the investigated features was the source, or the main cause, of the compromised state of the washing module.

Discussion

Due to the washing module's persistent condition of fluid flow inhibition, it was determined that the source of its failure must be rooted in its fundamental design. The fundamental design pertains to the hydraulic manifold, which the system (washing module) is based off of. The fact that the solenoids were actuating correctly and all electrical and mechanical components of the module were properly joined and structurally stable led to the extrapolation that there was an inherent design flaw within the hydraulic manifold. The hydraulic manifold prototyping chapter discusses the inherent design flaw in further detail and explains the actions taken in order to solve the intrinsic defect.

Chapter 2: Prototyping of the Hydraulic Manifold

Introduction

This chapter discusses the prototyping of the hydraulic manifold that was performed in efforts to enable the isothermal titration calorimeter (ITC) to perform reliable and accurate thermodynamic data. The hydraulic manifold that is used within the washing module (Figure 5) of the ITC system is responsible for maintaining a clean environment within the injection syringe and sample and reference cells. The hydraulic manifold is also responsible for loading the substrate and delivering the testing buffer into the sample cell. Through maintaining a residue-free environment the hydraulic manifold increases the accuracy and precision of the thermodynamic data by removing any residue from prior tests that could add to the heats of the reaction. If any residue from a prior ITC test remains in the injection syringe or within the sample and/or reference cells the results of the ITC experiment, that is consecutively performed, will be compromised. The current hydraulic manifold that is used within the washing module has inherent design flaws that render the ITC unable to produce reliable and accurate data.

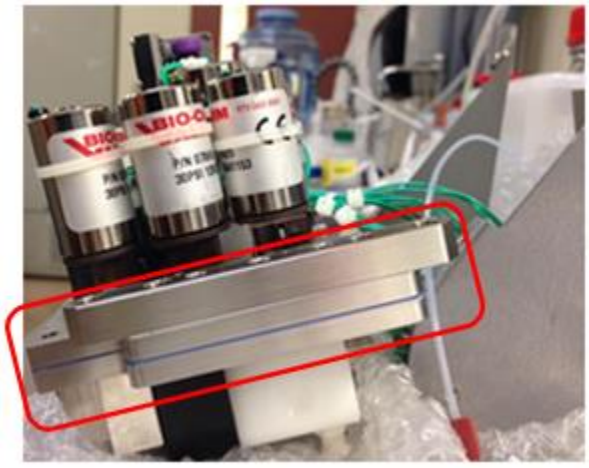

Figure 5. Internal components of MicroCal ITC200 washing module. Image of the internals of the washing module illustrating the original hydraulic manifold outlined in red.

The current washing module for the ITC has an internal suction pump which screws into the hydraulic manifold and is the source of the current design flaw. The length of the screws responsible to connect the internal suction pump and hydraulic manifold are too long which, over time, will puncture the silicon gasket as seen in Figure 6. After the rupture of the silicon gasket, the hydraulic manifold is unable to generate positive and negative pressure which is required in order to generate fluid flow. Once the washing module can no longer generate fluid flow the module is unable to create an adequate testing environment for the ITC; rendering the system inoperative. Therefore the need to create a hydraulic manifold that can have a longer operating life (the current operating life of the hydraulic manifold is around two years) is imperative.

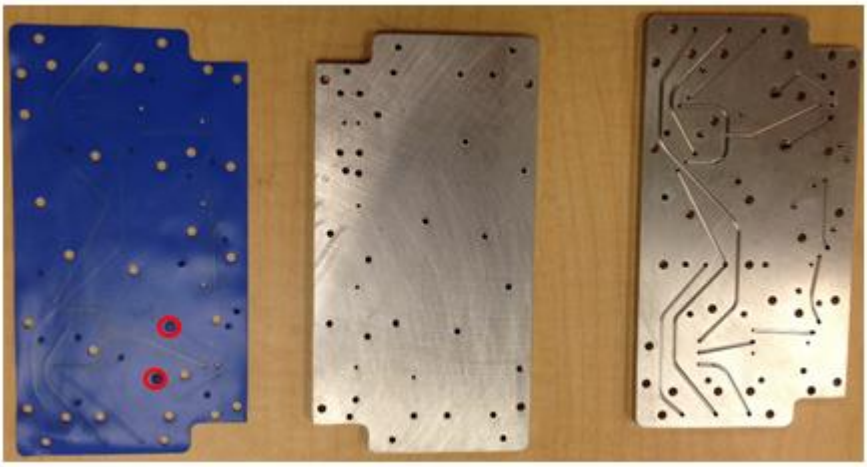

Figure 6. Image of the three components of the original hydraulic manifold after initial separation of the manifold. The three components of the hydraulic manifold are: silicon gasket (left), front plate (middle), and back plate which has the microchannels on the inner side (right). The puncture of the silicon gasket (main design flaw) is shown by in red circles.

Details of Key Constraints

In order to design a hydraulic manifold that can operate successfully and maintain the needed testing environment of the ITC, knowledge of the current design of the hydraulic manifold is imperative. Due to the regulation of the washing module by GE Healthcare, the main provider of the entire system, the engineering drawings and specifications of the washing module is inaccessible. In order to learn about the design of the hydraulic manifold we separated the front and back plate using a mechanical advantage technique.

Once the manifold was apart the design of the internal microchannels and silicon gasket became known (figure 2).

The available resources in order to fabricate the prototypes of the hydraulic manifold were a limiting factor in the progress of development. The precision tooling that is needed in order to mill and extrude the screw holes and edges of the hydraulic manifold is extremely specific and unique in size. The end mill diameter needed in order to fabricate a prototype of the front plate of the hydraulic manifold is 0.0625" which requires the use of a material that will not be too soft but maintain the structural integrity needed. The availability of polymers that would suffice for recreating a hydraulic manifold was also limited due to time. In order to develop prototypes as quick as possible we limited our material selection to what we could purchase at local polymer retail centers.

Design Description

To alleviate the hydraulic manifold of the current design flaw we redesigned the front plate of the manifold in a CAD program and fabricated three prototypes out of two polymers (figure 3, 4, and 5). The three prototypes were only of the front plate of the hydraulic manifold in order to prove that the prototype would work with the microchannels and solenoid design. This would remove the need for a silicon gasket and in essence solve the design flaw of the internal suction pump's screw length. With the removal of the silicon gasket the screws of the internal suction pump would have nothing to puncture which would increase the useful life of the hydraulic manifold.

In order to design the original hydraulic manifold we laser scanned both sides of the front and back plate and imported the images into Inventor 2015. Once the image was in Inventor the dimensioning of all the screw and fluid holes as well as the size of the manifold was performed with a final tolerance of 0.001". In order to verify that the CAD drawings were accurate, the first prototype of the hydraulic manifold front plate was fabricated out of high density polyethylene (HDPE) obtained from Tap Plastics (Figure 7).

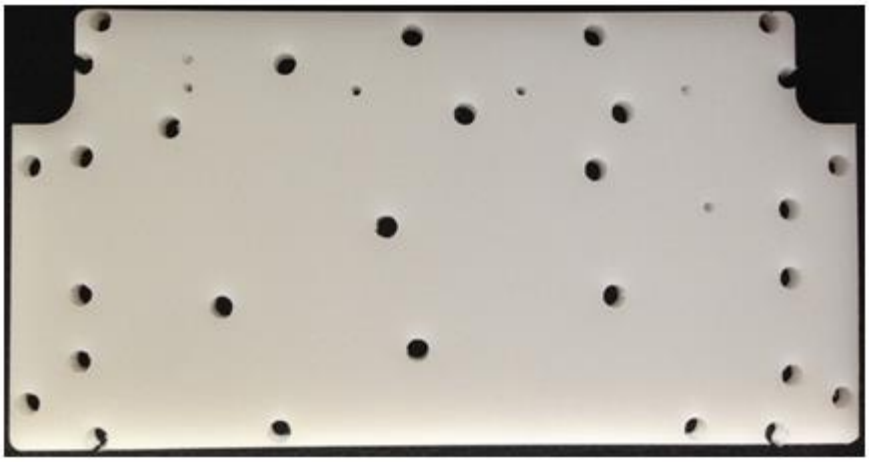

Figure 7. Prototype 1 made out of high density polyethylene (HDPE). The perimeter of HDPE back plate has incomplete screw holes. Prototype was made with a laser cutting machine with a tolerance of 0.001”. Incomplete screw holes is due to the diameter of the laser cutting tool being slightly larger than the desired screw holes.

Figure 8. Prototype 2 made out of high density polyethylene (HDPE). The perimeter of HDPE back plate has incomplete screw holes. Prototype was made with a laser cutting machine with a tolerance of 0.001”. Incomplete screw holes is due a lack of HDPE resulting in a smaller width than desired.

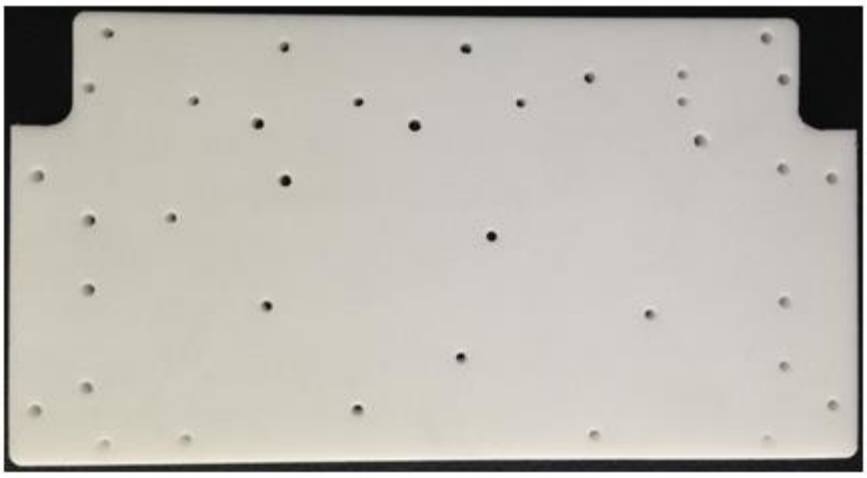

Figure 9. Prototype 3 made out of polytetrafluoroethylene (PTFE, Teflon). This prototype shows successful fabrication without openings in the screw holes along the perimeter.

Once the HDPE was obtained a CNC mill was used in order to create the CAD designed front plate of the hydraulic manifold. HDPE was used as the material for the first prototype because of its easy to machine characteristics as well as the characteristics that are outlined in Table 6. The polymer is relatively soft which would allow for the CNC machine to easily fabricate the manifold. After machining the HDPE prototype, the perimeter was breached in a few areas due a miscalculation in the CAD drawing (Figure 10). The diagram of the hydraulic manifold was then adjusted and development of the second prototype on HDPE was performed. The purpose of the second prototype was to further verify and confirm that the dimension of the CAD drawing was correct.

Table 6: HDPE characteristics

Property	Type	Unit	HDPE
Mechanical	Compressive Strength	Psi	2700 – 3600
	Hardness	Shore	D60 – D70
	Coefficient of Friction	Against Polished Steel	0.20
Chemical	H_2O Absorption	% in 24 hrs.	Low < 0.01
	Solvent Resistance	Degrees C (^oC)	< 60 ^oC
	Acid Resistance	-	Oxidizing Acids
	Alcohol Resistance	Methyl alcohol (100 %)	Satisfactory

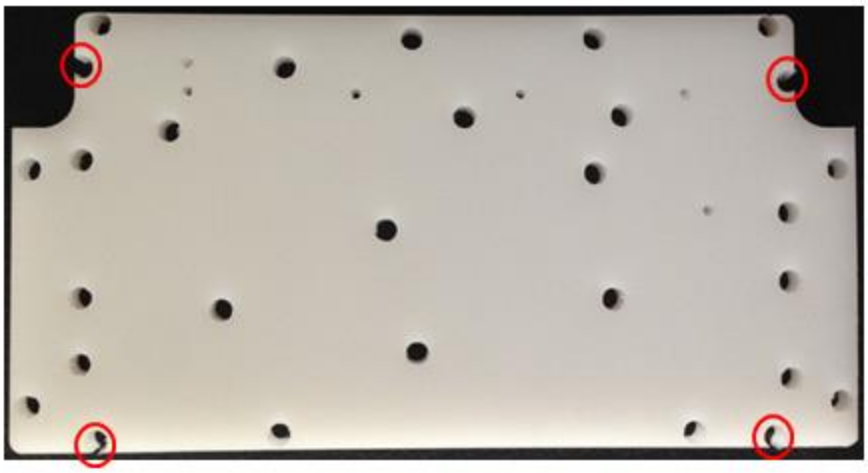

Figure 10. Prototype 1 made out of HDPE. This prototype contains the incomplete structural screw holes outlined in red.

After the CAD drawing was completely accurate and took into account the CNC end mill's tooling diameter, the third prototype was ready to be fabricated (Figure 9). The material that the third prototype was fabricated out of was polytetrafluoroethylene (PTFE, "Teflon"). The material characteristics described in Table 7 point out the superior features that PTFE possesses. PTFE's low coefficient of friction, 0.05-0.08, would decrease the flow resistance that would occur inside the hydraulic manifold's microchannels allowing for the internal suction pump to be more efficacious in its power conversion. Complementing the low coefficient of friction of PTFE is the hydrophobic nature of the material's molecular structure (Figure 11). The carbon-fluorine interaction is highly electronegative which influences its low susceptibility to brief dipoles and, as a result, increases the hydrophobic nature of the molecules. The more hydrophobic the material is the lower coefficient of friction the material will have. The PTFE is also chemically inert. The strength and stability of the interaction between the carbon and fluorine result in the material having an extremely low chemical reactivity to alcohol and corrosive substances. This chemical inert feature that PTFE possesses would increase the usable life of the prototype; a driving force for the decision to utilize PTFE as the prototype material or the front plate prototype. In addition to PTFE's chemical stability, the material contains the ability to slightly conform under compression. The conforming characteristic of PTFE allows for the material to act as a self-seal which removed the

need for the silicon seal. Without the silicon seal, the length of the internal suction pump's screws would not puncture the gasket and in effect solve the inherent design flaw of the original hydraulic manifold.

Table 7: PTFE characteristics

Property	Type	Unit	PTFE
Mechanical	Compressive Strength	Psi	3500
	Hardness	Shore	D50 – D65
	Coefficient of Friction	Against Polished Steel	0.05 – 0.08
Chemical	H_2O Absorption	% in 24 hrs.	< 0.01
	Solvent Resistance	-	Excellent
	Acid Resistance	-	Inert
	Alcohol Resistance	Methyl alcohol (100 %)	Satisfactory

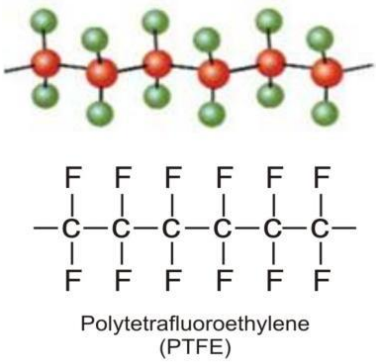

Figure 11. PTFE's molecular structure. Adapted from Anticorrosive Equipment Pvt. Ltd.

Detailed Analysis

The design criteria for the hydraulic manifold's front plate prototypes were that they needed to have the structural support, chemical stability, hydrophobic nature, and, most importantly, the ability to remove the need for the silicon gasket. The surface of the HDPE prototypes can be treated with heat that will allow for the material to conform and act as a self-seal which qualified it for the use of a prototype. The availability and ease to machine aspects of the HDPE also greatly influenced the application of the material for

the first and second prototype. The first and second prototype (figures 3 and 4) improved the accuracy of the CAD drawings through having the perimeter of the prototypes being breached by the tooling diameter of the end mill. After the adjustment of the diameter of the screw and fluid holes in Inventor, the CAD drawing had a tolerance of 0.001" and was accurate enough to be fabricated without any breaches of the perimeter.

At the time when the first two prototypes were completed, PTFE was available and was used as the third prototype. The fabrication of the PTFE prototype was flawless with the adjusted CAD drawing. However, there was an unexpected occurrence when the steel back plate was screwed to the PTFE front plate. After assembly of the washing module, fluid flow testing began but the result was unsatisfactory. Fluid flow remained dormant demonstrating that the PTFE prototype was unsuccessful. The conforming characteristic of PTFE was a great motivational factor to implement the material for prototyping, but the conforming nature of PTFE proved insufficient to act as a seal for the hydraulic manifold. The manifold had leaks where the PTFE did not conform adequately. Leaks in the hydraulic manifold inhibited the ability of the system to generate sufficient positive and negative pressure that is necessary for fluid flow.

Expected results

When creating the initial CAD drawing which was to be used in order to fabricate the first HDPE prototype, it was assumed that the dimensioning was correct. Through the fabrication process involving the CNC mill machine the actual results of the first HDPE prototype did not mirror the assumption. After fabrication of the first prototype the calculation error involved in the perimeter screw holes became apparent. The perimeter of the first HDPE prototype was breached by the greater diameter of the end mill compared to the diameter of the perimeter screw holes in the CAD drawing. The prototype did not meet the requirement of being a functional front plate to the hydraulic manifold. However, the necessary increase of perimeter screws' diameters was realized through the construction of this prototype.

Once the CAD drawing was adjusted in order to better reflect the diameter of the end mill, the second prototype with HDPE was generated. The result of the second prototype was expected to be that the HDPE hydraulic manifold front plate would be assembled to the back plate and initial testing would take place. When cutting and milling the second prototype, however, the requirement that the prototype should be a functional front plate for the hydraulic manifold was not fulfilled. The failure of the second prototype was not due to the dimensioning of the front plate on the CAD drawing but due to a lack of material. The sheet of HDPE proved to be slightly too small in length and width. The lack of material for the second HDPE prototype resulted in the breaching of a few sections of the perimeter which rendered the prototype dysfunctional.

When the second HDPE prototype failed, the desired material, PTFE, was available and the third prototype was created. It was expected that the third prototype would be correctly dimensioned and that the assembly of the washing module with the new hydraulic manifold would operate correctly. The conforming nature of PTFE was expected to provide an adequate self-seal and the hydraulic manifold was expected to be able to create positive and negative pressure. The expectation that the PTFE prototype would be able to generate positive and negative pressure influenced the belief that the washing module would generate fluid flow and would adequately clean the injection syringe and sample and reference cell. After fabrication of the PTFE front plate prototype and assembly of the washing module, fluid remained stationary resulting in the system being debilitated.

Back-Up plan

A contingency plan was developed in the event that the PTFE prototype failed in serving as an adequate front plate and gasket to the hydraulic manifold. The design of the fourth prototype was uniquely different from the past three prototypes. Instead of working to fabricate half of the hydraulic manifold the fourth prototype would serve as the entire hydraulic manifold. The design focus for the fourth prototype is to find a material that is structurally stable under compressive force and has the characteristic to bond with itself.

The material that fit both of the design criteria (rigid in structure and can bond with itself) was polycarbonate. The characteristics of polycarbonate that were the most favorable were the hardness (M70) and the alcohol and acid resistance (good) as shown in Table 8.

Table 8: Polycarbonate characteristics

Property	Type	Unit	PTFE
Mechanical	Compressive Strength	MPa	> 80
	Hardness	Rockwell	M70
	Coefficient of Friction	-	0.31
Chemical	H_2O Absorption	% in 24 hrs.	0.01
	Acid Resistance	-	Good
	Alcohol Resistance	-	Good

Polycarbonate can be utilized with a PTFE bonding agent which would allow the material to fuse together. The PTFE bonding agent could be applied to the polycarbonate which would cause the surface of the polycarbonate to melt and then quickly solidify. With the application of the PTFE bonding agent around both sides of the microchannels of the hydraulic manifold's back plate and consecutively aligning and compressing the front plate to the back plate, the two inner surfaces of the two pieces of the hydraulic manifold would melt and quickly solidify essentially rendering the manifold one piece. Creating a hydraulic manifold that acts like a single piece would render it a closed system and alleviated any possible leaks within the manifold. This would allow the hydraulic manifold to create positive and negative pressure for fluid flow, enabling the washing module to provide a clean testing environment for the ITC.

In order to take into consideration the possible overspill of the PTFE bonding agent into the microchannels, the CAD software was adjusted accordingly. Specifically the CAD drawing contained deeper microchannels such that the possible overflow of PTFE bonding agent would not inhibit fluid flow. When utilizing the PTFE bonding agent in order to render the hydraulic manifold a closed system, there would be no need for the structural screws on the original CAD design. Increasing the available space in the manifold would allow for the redesign of the microchannels which led to a more linear microchannel design instead of the current design that exhibits hard angles and long

channels (Figures 12 and 13). Therefore utilizing polycarbonate as a fourth prototype material in order to fabricate the entire hydraulic manifold proved, theoretically, as a promising future step.

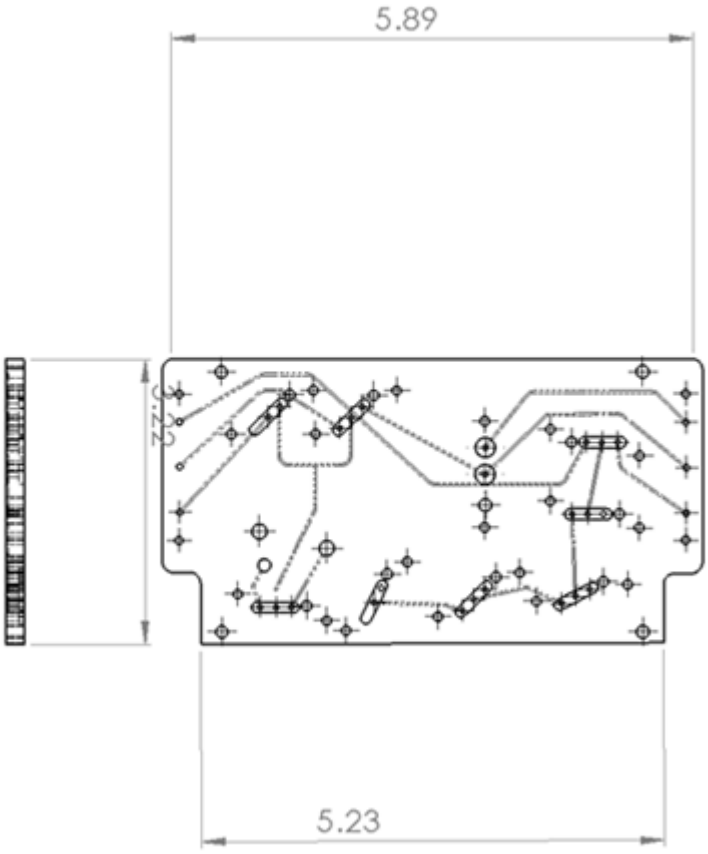

Figure 12. Dimensions of the perimeter of the hydraulic manifold performed on the CAD software. The design is for the future polycarbonate prototype and has the structural screws from the original design removed.

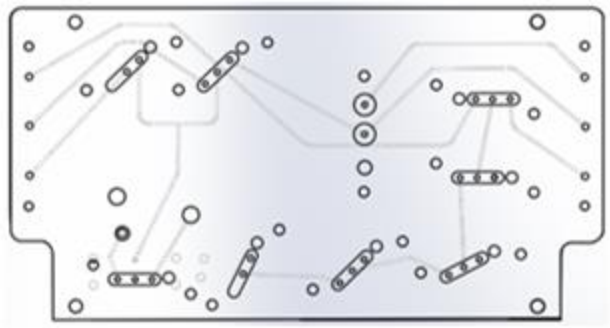

Figure 13: Illustration of the design of the polycarbonate prototype for future fabrication. The structural screws have been removed in order for the redesign of the microchannels to be possible. The viewpoint is from a bird's eye view of the back plate with the material being translucent in order to show the orientation of the microchannels within the hydraulic manifold.

Materials & Methods

The materials used in order to create the three prototypes are listed in Table 9.

Table 9. Description of the prototype number and the material used for fabrication.

PROTOTYPE	MATERIAL
Prototype 1	High Density Polyethylene
Prototype 2	High Density Polyethylene
Prototype 3	Polytetrafluoroethylene, Teflon

The tools and materials that were utilized in order to create the three prototypes are illustrated in Table 10 along with the quantities of the materials.

Table 10. Explanation of the material and tools used in order to fabricate the three hydraulic manifold front plate prototypes.

TOOL / MATERIAL	QUANTITY
PTFE (Teflon) sheet, 6.5" x 48"	1
HDPE (high density polyethylene) sheet, 12.5" x 13"	1
Two flute steel and carbide coated end mill, 0.0625" diameter	1
3 axis CNC milling machine	1
Safety goggles	1
3-Dimensional scanner	1

CAD software (Autodesk Inventor 2015 and or, SolidWorks Professional 2014	1 license
Flash drive (minimum memory of 500 megabytes)	1
Tool path and G-code generator (VCarve Pro and or BobCAD-CAM)	1 license

The procedure that was utilized in order to develop the hydraulic manifold front plate prototypes was as follows:

1. Extract steel hydraulic manifold, front and back plate.
2. Use 3-dimensional scanner to generate image of the manifold.
3. Open the image file generated by the 3-D scanner using CAD software, such as SolidWorks, or Autodesk Inventor.
4. Using the CAD software, generate a 3-D model of the steel hydraulic manifold, include both the front and back plates. Note that the front and back plates of the hydraulic manifold are two separate parts, each with two sides that must be illustrated precisely in the software program.
5. After the model is generated, use the software's integrated dimensioning tools to accurately record the dimensions and features of the manifold. Identify the length, width, depth of extruded features, thickness of the material, and the diameter and placement of all the holes and features.
6. Save the front and back plate hydraulic manifold files as separate components using descriptive titles to distinguish between the components.
7. Create an assembly file using both the front and back manifold components to make sure that all holes and edges are perfectly aligned. This alignment process is done using the constrain features integrated into both SolidWorks and Autodesk Inventor.
8. Review and compare dimensions and features of the assembly and component files to the physical steel hydraulic manifold's front and back plate that were scanned using the 3-D scanner earlier to check that the files in the software match up with the physical manifold.

9. After review, open the component file for the front plate of the manifold and export the top and bottom faces as a DXF file to a separate folder. Repeat this step for the both plates of the manifold.
10. Using CAM software like VCarve Pro or BobCAD-CAM, open the DXF files for the top and bottom face of the front plate of the hydraulic manifold.
11. Select vectors, and create tool path.
12. Input the cutting specifications (as listed below in Table 11) into the software's required fields to define what tool and material will be machined.
13. Save the G-code to a file on your flash drive and insert the flash drive into the CNC mill.
14. Before milling be sure to wear safety goggles and have compressed air to shoot chips away from the cutting tool while milling.
15. Secure materials to the work area one at a time using specified work holders (such as a vice).
16. Make sure to manually set the machine's zero for its x, y, and z axis's.
17. Finally run the G-code using the BobCAD-CAM CNC controller and pay close attention to the end mill as it cuts through the material. Repeat these steps for each piece of material (HDPE and PTFE).

Table 11: Details of the specifications and dimensions for each specification in regards to both prototyping materials.

SPECIFICATION	**DIMENSION**	
	HDPE Prototype	PTFE Prototype
Tool type	PTFE (Teflon) sheet, 6.5" x 48"	1
Tool Diameter	2 flute high speed steel	2 flute high speed steel
Pass Depth	0.03125 inches	0.0125 inches
Step Over	0.0125 inches	0.03125 inches
Spindle Speed	6,000 rpm	14,000 rpm
Feed Rate	200 ipm	400 ipm
Plunge Rate (for drilling)	0.125 inches	0.125 inches
Tabs	2	2

Results

Despite the completion of three prototypes in efforts to fabricate a front plate for the hydraulic manifold for the MicroCal ITC 200 Washing Module, the goal to render a functional system was unsuccessful. The first HDPE prototype proved to have inadequate dimensions for the screws along the perimeter of the CAD drawing, and, as such, when tooling the HDPE front plate, the end mill's diameter was greater than that of the screw hole's diameter, causing breaches in the perimeter.

The second HDPE prototype was constructed adjusting the diameter of the screw holes along the perimeter of the front plate in the CAD drawing. Due to a lack of material, the HDPE sheet was slightly too thin and too short and this rendered the perimeter of the second prototype open at various points.

The third prototype made out of PTFE proved to be the most promising front plate to render the hydraulic manifold functional, but followed suit with the two HDPE prototypes. The PTFE prototype was the only front plate to be fabricated correctly and successfully assembled with the original steel back plate. Once the washing module was turned on and cleaning tests were performed, the washing module remained unable to generate fluid flow.

Discussion

The failure of the first two hydraulic manifold front plate prototypes made out of HDPE occurred due to a miscalculation and an inadequate supply of material. When designing the front plate of the manifold on Inventor, the dimensioning of the screw and fluid holes as well as the length and width of the front plate were performed to obtain values as close to the current front plate as possible (obtained a tolerance of 0.001"). When it was time to fabricate the front plate the diameter of the end mill was larger than that of the diameter of the screw holes along the perimeter of the front plate. This caused the first prototype to fail and have openings along the perimeter. Although the first prototype failed, the fabrication of the prototype revealed the need to adjust the dimensions of the CAD drawing to account for the tooling diameter which is essential when generating prototypes.

After adjusting the CAD drawing and creating the second HDPE prototype various openings in the front plate perimeter continued to exist. The breaches in the perimeter of the second HDPE prototype were not due to an incorrect dimensioning of screw holes in the CAD program, but due to the time sensitive nature of generating a functional front plate that could render the washing module functional and provide the necessary sterile injection syringe and sample and reference cell of the ITC such that reliable and accurate thermodynamic data could be achieved. The pressure to create a functional hydraulic manifold led to the decision to adjust the CAD drawing to account for the tooling diameter and then immediately machine the HDPE sheet. The result of this was that the HDPE sheet was inadequate in size and led to openings in the perimeter at various points which rendered the front plate inoperable. Making a time sensitive decision led to the fabrication of an inadequate front plate but because of this decision the fabrication of the following prototype did not occur without great thought and consideration for possible flaws.

The third and final prototype, the PTFE front plate, proved to be the most promising but inadequate to use as a front plate for a hydraulic manifold, as PTFE's conforming property was insufficient for the purpose of a hydraulic manifold gasket. After assembly of the front and black plate of the hydraulic manifold (Figure 14) the washing module was unable to generate fluid flow due to the leaks in the hydraulic manifold where the PTFE did not conform enough around the perimeter. In addition the screws that went through the PTFE front plate were not air tight due to the inadequate hardness of the PTFE.

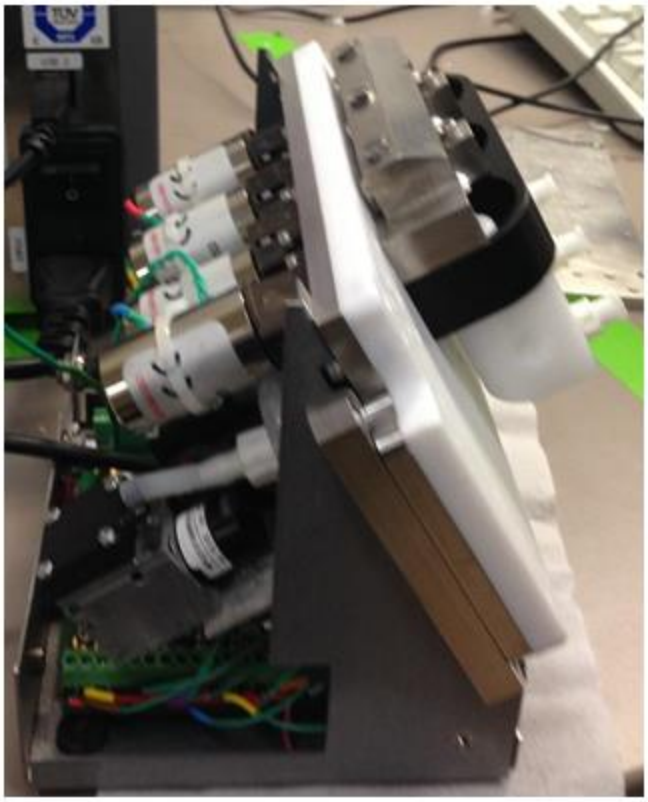

Figure 14. Illustration of the assembly of the PTFE front plate with the steel back plate.

The overall fabrication and results of the PTFE prototype provided as a lesson in which a theoretically promising material was inadequate after implementation. The hardness property of the PTFE was the down fall of the material which inhibited the hydraulic manifold of being air tight. Fabrication of the PTFE prototype, as well as the two HDPE prototypes developed the engineering design and thought process of this issue. As such, a better understanding of the system was gained in order to design and plan future prototypes.

Chapter 3: Pyridostigmine Bromide

Introduction

In this chapter we will present the results of our ITC experimentation. As mentioned, we thank Dr. Daryl Eggers, for the experiments were carried out in his laboratory at San Jose State University using a MicroCal VP-ITC. This is a larger version ITC than the one we are working on and that is housed at Santa Clara University. Our lead drug candidate for our design project was a molecule by the name of pyridostigmine bromide (PB). PB is a current prescription drug used to improve muscle strength in patients with myasthenia gravis, a muscular disease. Our collection of results will be discussed herein, as well as current hypotheses we have surrounding the data.

There is no previous research to date describing the physical interaction between SrtA and PB. To reiterate, PB was produced as a drug candidate via a high-throughput screening assay performed in house that measured its ability to inhibit SrtA activity. PB was selected as the leading drug candidate because of its chemical structure. The ester bond and aromatic ring present in PB's chemical structure give it an appealing likeness to the structure of an amino acid (Figure 15).

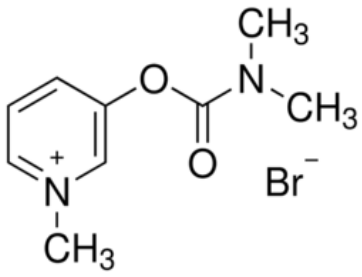

Figure 15. Chemical Structure of Pyridostigmine Bromide

SrtA cleaves an ester bond between a threonine and glycine on its LPXTG substrate in nature. As such, it is hypothesized that SrtA may cleave PB in a similar fashion.

ITC is a popular instrument for drug discovery projects, and we find it a suitable method for furthering our understanding of the interaction under study. Simpler methods can show that PB inhibits SrtA (see Literature Review section), but gaining a greater understanding of the SrtA-PB physical interaction will bring us closer to grasping the

exact mechanism of interaction. Through ITC, we can also determine how strong the interaction is, which, in turn, has a direct correlation to its ability to be carried forward as a serious drug candidate.

Details of Key Constraints

The key constraints to any ITC experiment are sample consumption and high sample concentration requirements. This was especially an issue because of the large volume requirement of the MicroCal VP-ITC at San Jose State University. Having our protein purification optimized and utilized for the MicroCal iTC200 (which has a much smaller volume requirement) resulted in using much more dilute solutions of SrtA. In general, higher concentrations lead to higher heats, which are easier for the instrument to detect, measure, and report.

Experimental Design

Negative Control

Our first titration was a negative control experiment – a reaction in which we did not expect to observe heats of binding. For this experiment, a solution of PB in HEPES buffer (our chosen aqueous buffer) was titrated into HEPES buffer. The buffers were matched (i.e. equivalent pH, salt content, HEPES concentration) so that there were no variables in the experiment except for the presence of PB in the titrant.

Positive Control

We set out next to produce a positive control experiment – a reaction in which we expected to observe heats of binding. For this experiment, we titrated a solution of SrtA's natural substrate, the five amino acid sequence LPETG, into a solution of SrtA. Both the substrate and SrtA were dissolved in the same HEPES buffer, and the buffers were matched. In this way, all that was observed in the reaction heat profile was the interaction between SrtA and its substrate.

PB Titration

Upon completing our controls, we had enough information to move forward and titrate with PB, our drug candidate. Both PB and SrtA were dissolved in HEPES buffer (matched) so that the only variables in solution were PB and SrtA. Based on a set of basic ITC guidelines, we took the concentration of SrtA that we purified and multiplied it by a factor of 15 to determine the concentration of PB with which to titrate. Using a 15-fold excess is generally a good place to start because it is ideal to be able to observe saturation of the protein if there is binding occurring. Then, based on the outcome of the first experiment, it is possible to adjust the concentrations for the next one to improve the appearance of the data and gain better fitting parameters.

Supporting Analyses

In order to determine all buffers were matched, stock solutions were made and adjusted to a uniform pH of 8.0. In addition, all protein solutions were dialyzed in the same buffer used to dissolve PB. These steps helped to ensure that the heats observed during the experiment would be due solely to the interaction between SrtA and PB. An important characteristic of ITC is that it displays the aggregate of what is occurring in solution. Because of this, researchers cannot say for sure that they are observing an interaction between their two molecules under study unless they know for sure that nothing else occurring in solution is producing any heat.

Expected Results

Negative Control

In our negative control we did not expect to observe heats of binding. However, we do expect to see some small heats released during each injection. This is solely the heat produced by diluting one solution into another; it is referred to as the ‘heat of dilution’. The way to distinguish between these kinds of heats and heats of binding is by first

looking at the magnitude of the heats, and then by looking at the binding isotherm. If each injection produces a peak of the same size, then the heat produced must be irrespective of anything present in solution. Therefore, small peaks that are equal in size over the course of the titration are an expected outcome of a negative control.

Positive Control

For our positive control, we expect to observe heats of binding. However, it is not certain how strong of an interaction there is between SrtA and its substrate, as there is conflicting data on the matter. Regardless, a positive control also affirms that the protein we purify is active and of high quality and purity. Further, we expect to observe a release of heat as a by-product of SrtA interacting with its substrate. Almost all binding events are exothermic in nature, so we expect to observe downward-facing peaks.

PB Titration

Given that the interaction between PB and SrtA has not previously been studied, this is an experiment with relatively few expectations. The important thing in this study is to be able to distinguish a non-binding event from a binding event. If PB does in fact bind to SrtA, we expect to observe exothermic peaks, as almost all enzyme inhibition reactions are carried out exothermically, that is, by releasing heat as a by-product.

Materials & Methods

Protein Purification

1. Induction:

Genetic material that codes for the SrtA protein was stored as DNA and kept in a freezer at -80°C. A small amount of this DNA was then transformed into competent *Escherichia coli (E. coli)* cells, allowing for the plasmid to be incorporated into the bacterial cells, and stored in a 50% glycerol solution at -80°C as well. By doing this, the DNA that codes for SrtA was taken up by bacterial cells (*E. coli*), which, when grown, transcribed and translated the DNA into the SrtA protein structure using its own cell machinery. The SrtA

DNA also encoded antibiotic resistance to an antibiotic called Kanamycin, rendering the *E. coli* cells resistant to Kanamycin. A small amount of this glycerol stock was inoculated in a 10mL solution of growth media, luria broth (LB), which contains the essential nutrients for bacterial growth. Kanamycin was also added to the solution to prevent the growth of other bacteria. This 10mL culture was inoculated overnight at 37°C. One liter of LB was prepared and autoclaved, and the 10mL culture was added to the 1L culture the next morning to induce further cell growth. An additional 1mL of Kanamycin was added to prevent bacterial growth other than the *E. coli* cells expressing SrtA.

This culture was grown to an optical density (OD_{600}) of 0.6. At this point, to further induce cell growth, 1mL of isopropyl β-D-1-thiogalactopyranoside (IPTG) was added. IPTG mimics a substance that induces transcription of a certain operon, the *lac* operon, which is contained in the plasmid harboring the SrtA gene. The culture was left to grow and induce for 6-8 hours. After induction, the cells were harvested using the Avanti J-26 XP centrifuge by Beckman Coulter, spun at 5,000rpm for 10 minutes. The supernatant was discarded and the wet weight of the cell pellet was measured. The pellets were stored at -80°C overnight.

2. Sonication:

The frozen cell pellet was thawed on ice and resuspended in of 4mL of lysis buffer (50mM NaH_2PO_4, 300mM NaCl, 10mM imidazole, 1mg/mL lysozyme) per milligram of cell pellet wet weight to lyse the cells. Sonication using the Sonic Dismembrator by Fisher Scientific was used to further lyse the cells in each sample, and the lysates were then centrifuged to sediment the cellular debris for 40 minutes at 16,000rpm in the Avanti J-26 XP centrifuge by Beckman Coulter. The supernatant was transferred to a centrifuge tube.

3. Purification:

A 1.5mL aliquot of Ni-NTA beads was washed with wash buffer (50mM NaH_2PO_4, 300mM NaCl, 20mM imidazole). To bind the proteins to the beads, the supernatant was added to the beads and was left to tilt on the Vari-Mix rocker by Thermolyne for two hours at 4°C. Ni-NTA beads bound to the C-terminal Histidine-tag of SrtA with

micromolar affinity. After binding, the SrtA-Ni-NTA bead mixture was washed with the same wash buffer - a phosphate buffer which helped to remove proteins that do not specifically bind with nickel ions. This process isolated the desired protein as it was the only one bound to the nickel ions in the bead mixture. The isolated SrtA was eluted from the beads using elution buffer (50mM NaH_2PO_4, 300mM NaCl, 250mM imidazole) containing a higher amount of imidazole which detaches the SrtA protein from the Ni-NTA beads.

4. Concentration and Dialysis:

Following elution there is generally 6-10mL of dilute protein solution. In order to increase the efficacy of the ITC experiment, as suggested earlier, a higher concentration is ideal. The final solution is concentrated down to approximately 3-4mL by centrifugation and dialyzed into 25mM HEPES buffer containing 2mM CaCl. As described previously, calcium has been shown to be essential for SrtA activity. Following dialysis, the protein is ready for ITC experimentation.

SrtA Substrate Solution Preparation

For our positive control, the five amino acid sequence LPETG was dissolved in 100% DMSO initially because it is not water soluble. DMSO is a well-known solvent, used especially in cases when solutes are not particularly hydrophilic. It was then diluted with HEPES buffer to its final concentration.

PB Solution Preparation

Another advantage of pyridostigmine bromide is its water solubility. As such, a 50 mM stock solution of PB in HEPES buffer was created. This solution was then diluted according to the optimal concentration for ITC analysis, which varied according to the concentration of protein available.

MicroCal VP-ITC Titration

The SrtA and PB solutions were transported on ice to San Jose State University each time an experiment was run. Once inside the laboratory, the two samples were degassed for

five minutes, and then the PB was loaded into the injection syringe. The VP-ITC sample cell was rinsed with HEPES buffer before the SrtA solution was ultimately added to the emptied cell.

Results

Negative Control

As previously described, our negative control was carried out by titration of a solution of PB in HEPES buffer into HEPES buffer (Figure 16). The titration was comprised of 54 injections of 5 microliters of our solution of PB into our buffer.

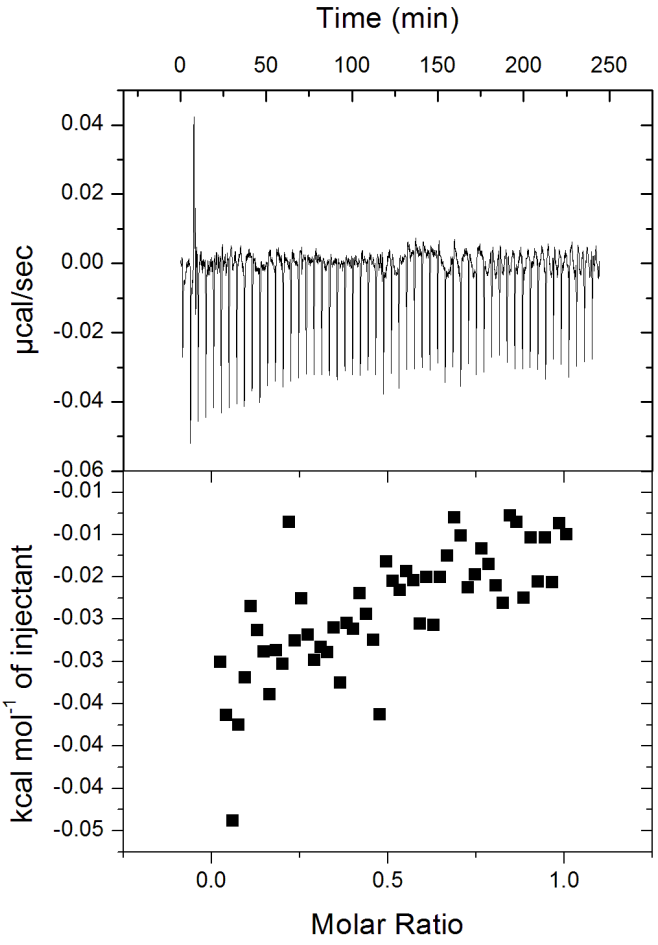

Figure 16. ITC Final Figure of PB into buffer. The graph at the top displays the raw data of the titration. The graph at the bottom displays the integrated data points, generated by the ORIGIN software.

Positive Control

The positive control was completed using 54 injections of 5 microliters of our SrtA substrate solution into a solution of SrtA. Due to the interaction between SrtA and its substrate, the heat changes were much larger than our negative control (Figure 17).

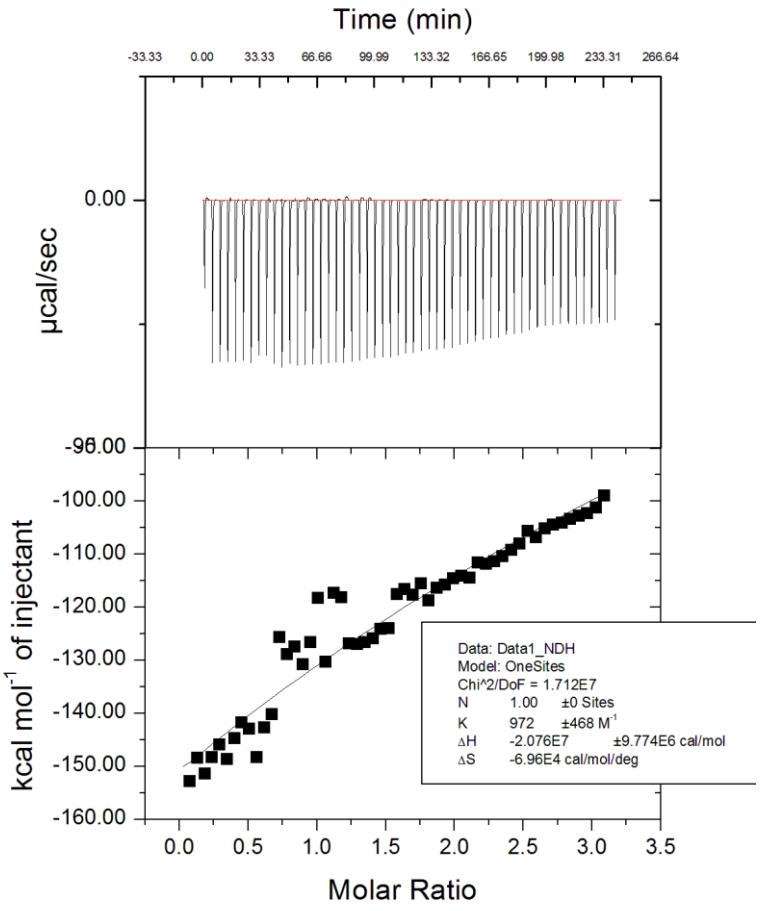

Figure 17. ITC Final Figure of SrtA substrate with SrtA. The graph at the top displays the raw data of the titration. The graph at the bottom displays the integrated data points, generated by the ORIGIN software. In addition, the integrated data was curve fitted using the ORIGIN software.

Due to the presence of heats of binding, the data was curve fitted to gain information on the strength of the binding reaction, as measured by the ITC. At low concentrations of protein, it has been shown that the least-squares estimate of the binding constant, K, is

virtually independent of errors in the stoichiometry parameter N [6]. This allows an accurate determination of K by freezing the stoichiometry parameter at N=1 (for a 1:1 binding system). Our curve fitting was carried out in this fashion since we expect SrtA to bind its substrate 1:1.

PB Titrations

The first titration with PB and SrtA used a concentration of PB 15 times greater than that of SrtA. Since we were expecting a low heat signal, we titrated with 15 microliter injections (as opposed to the standard 5 microliters), which reduced our maximum number of injections down to 17 (Figure 18).

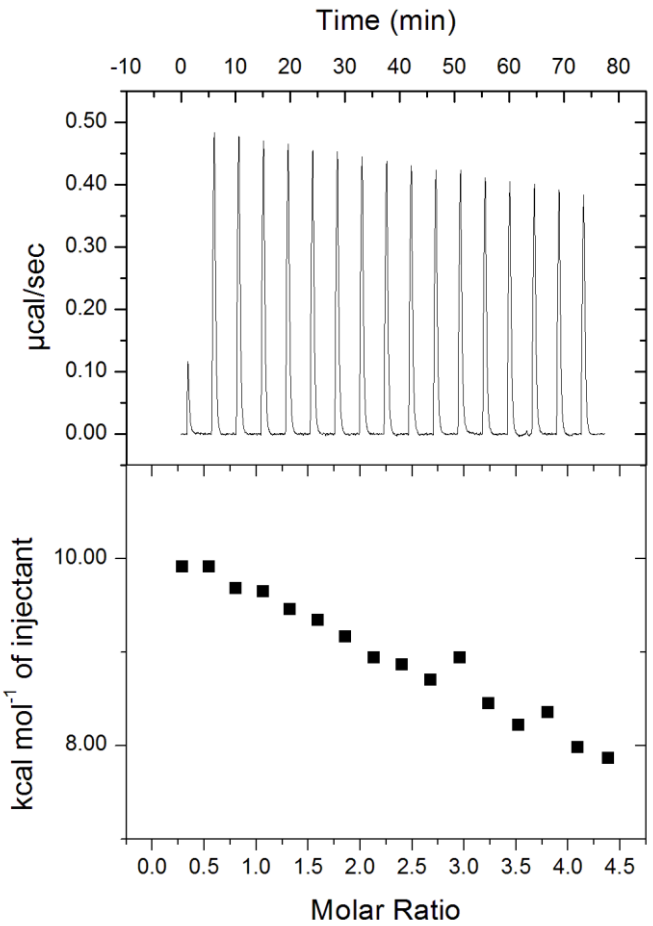

Figure 18. ITC Final Figure of PB with SrtA. The graph at the top displays the raw data of the titration. The graph at the bottom displays the integrated data points, generated by the ORIGIN software.

In the raw data for this titration we observed the strange result of an apparent endothermic reaction. The positive-facing peaks indicate that the calorimeter feedback system had to supply more power to the sample cell because the reaction required heat from its environment, lowering the temperature of the cell. For reasons still under contemplation, the integrated data was not able to be curve fitted. Based on the shape of the raw data, it was gathered that the reaction had not reached saturation. We noted that while there was a small decline in heat absorbed with each injection, it was not nearly saturated.

We took this into account and performed a second titration of PB with SrtA, this time using twice as much PB (30X the concentration of SrtA). This was done in order to facilitate saturation by titrating with a large excess of PB. The titration that followed carried with it all of the same experimental conditions; only the concentration of PB was increased (Figure 19).

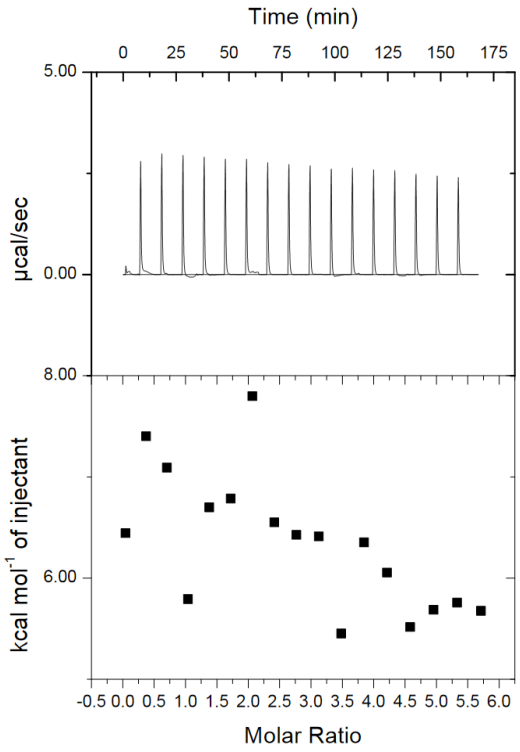

Figure 19. ITC Final Figure of second trial of PB with SrtA. The graph at the top displays the raw data of the titration. The graph at the bottom displays the integrated data points, generated by the ORIGIN software.

The first thing we noticed about the raw data of this titration was that it had a similar shape to the prior titration. Each injection also seemed to produce a much larger magnitude as far as heat absorbed. The positive-facing peaks again indicate the addition of heat to the sample cell.

Discussion

Negative Control

What we observed in the negative control was a sequence of minor downward-facing peaks (Figure 16). Based on the magnitude of the peaks, we safely concluded that no reaction is occurring. The effect seen was that of dilution: when one solution is diluted into another, there is a miniscule amount of heat given off as the solutions mix and come to equilibrium. In addition, small amounts of heat are picked up by the ITC based just on the physical nature of mixing one solution into another.

We are confident that the heats recognized are not heats of binding by two characteristics of the graph: (1) the magnitude of the injection peaks and (2) the way the magnitude of the peaks did not exhibit an appreciable change over the course of the titration. What we learn from the negative control experiment was that, in general, when PB is titrated into another solution (our buffer), no appreciable heat change is produced, either by reaction with the buffer salts or just having a high heat of dilution. The smaller the effect seen in a negative control, the easier it is to subtract from the eventual experimental data.

Positive Control

Our positive control verified for us that the SrtA we purified was active and pure. Based purely on the magnitude of the peaks in the raw data (Figure 17), we can conclude that a significant amount of heat has been released as a result of the addition of substrate to the solution of SrtA. By the shape of the overall titration, we can conclude that binding does occur. This is seen by the fact that as the titration progresses, smaller and smaller amounts of heat are generated by the binding reaction. This is because as the titration progresses, SrtA molecules become bound to its substrate. The effect is that there are fewer molecules of SrtA available to bind to the substrate upon each subsequent injection

of substrate. Additionally, the ORIGIN software was used to curve fit the integrated data. Through curve fitting the data, we were able to obtain a rough estimate of the binding affinity that SrtA has for its substrate. Our results show an approximate Kd (dissociation constant) of 1mM (this is the concentration of substrate at which half of the molecules of SrtA will be bound and half will be free in solution).

PB Titrations

Our initial observations of our titration with PB led us to believe that the reaction between SrtA and PB is endothermic. The upward-facing nature of the peaks indicates that heat is being supplied to the sample cell because it has undergone a drop in temperature. This means that the reaction requires the absorption of heat from its environment to proceed. This was a surprising event to observe because most enzyme-inhibitor reactions, and most binding reactions in general, are exothermic in nature. We asked ourselves how an endothermic reaction was occurring and performed a thermodynamic analysis. To determine if the reaction was spontaneous, that is, whether it proceeds naturally without the addition of energy, we looked at the Gibbs free energy equation (eq. 3).

$$\Delta G = \Delta H - T\Delta S \qquad \text{(eq. 3)}$$

A spontaneous reaction has a negative ΔG. Given that our observed reaction is endothermic, ΔH is positive. For ΔG to be negative while ΔH is positive, the term TΔS must be greater than ΔH. There is thus a temperature dependence on the spontaneity of the reaction. At high temperatures the reaction is spontaneous, and at low temperatures the reaction is non-spontaneous. We believe that the reaction is occurring spontaneously for the following reasons: non-spontaneous endothermic reactions can only generally take place if they are coupled to very large exothermic reactions, or if their products are quickly shuffled into subsequent exothermic reactions. However, if this were occurring, we would observe it in the ITC data. In fact, the large exothermic reaction would dominate the small endothermic reaction occurring and would mask the endothermic reaction. For these reasons, it follows that it is a spontaneous endothermic reaction. But again it is temperature-dependent; it can only proceed spontaneously at high

temperatures. In order for the TΔS term to be positive, ΔS must then also be positive. This is the change in entropy, and having a positive change in entropy means that there is an increase in entropy in the system. We do not yet have enough evidence to support the exact mechanism, however, we believe the reaction is governed by entropic forces. This is doubly interesting because not only do typical binding reactions proceed exothermically, they are also largely driven by changes in enthalpy (ΔH).

For reasons we are still discussing, the data was not able to be curve fitted by the ORIGIN software. However, we reminded ourselves of the observation that it appeared the reaction did not reach saturation. This was determined by the shape of the raw data, and noting that upon each subsequent injection of PB, a relatively similar magnitude of heat change was generated in the cell. When saturation occurs, injections at the end of the titration produce very little heat, and the heats begin to approach the "heats of dilution" obtained in the negative control.

Our next titration used twice the amount of PB as before to try to force the reaction to become saturated. It was our hope that by increasing the concentration, the SrtA in the sample cell would become saturated with PB sooner. What we ultimately saw was quite different than what we expected. There was virtually no change in the shape of the raw data, only a large difference in the magnitude was noted (which was expected). The increase in the magnitude of the heats per injection reflects the large increase in the number of moles of PB added to the solution at each injection. However, we observe in the data that by increasing the number of moles added at each injection, SrtA does not become saturated any more quickly than at a lower concentration.

One explanation for the lack of saturation is that the protein (SrtA) and the drug candidate (PB) could potentially be recycled after each injection, such that by the time a new injection begins, all the SrtA is just as free in solution as it was before the previous injection. This would imply a sort of transient binding reaction, one in which the ligand (PB) does not stay bound to SrtA for long periods of time. At present, we await further data before speculation is continued.

Summary & Conclusions

Future Work

Further research is necessary to continue to discover the compounds that inhibit SrtA and to design a hydraulic manifold that will maintain the sterile testing environment that is necessary for ITC experimentation. Through identifying Pyridostigmine Bromide as an inhibitor of SrtA and discovering that the binding between the compound and SrtA is endothermic, it is likely that the binding mechanism of SrtA is different, or that there is an alternative binding strategy, then that currently believed [8, 10]. Future research should investigate Pyridostigmine Bromide further for its binding characteristics in order to verify the binding mechanism that this unique compound employs to inhibit SrtA. In addition to studying the characteristics of Pyridostigmine Bromide, further experimentation with the molecules outlined in the budget should be investigated via ITC.

Polycarbonate proves to be a possible material that will suffice for the recreation of the hydraulic manifold, and should be further researched. The failure of PTFE led to the discovery that polycarbonate could be a viable material for the fabrication of the entire hydraulic manifold. It is suggested that the development of the polycarbonate manifold be designed without the structural screws that exist in the current design to allow for the redesign of the micro-channels. A new design of the micro-channels that decreases the angles and length of the channels to be more linear and direct can improve the efficiency of the internal suction pump and efficacy of the washing module to maintain a suitable environment for ITC experimentation. Utilizing polycarbonate, or an alternative material that can fuse to itself, the hydraulic manifold can be fabricated to act as one piece (by fusing the back and front plate together) which will decrease the possibility for leaks through the perimeter of the manifold. Although further prototyping is needed, polycarbonate proves to be a suitable starting point for further research.

Through the ITC experimentation and hydraulic manifold prototyping the research lessons learned have been immense. The unexpected binding data received from Pyridostigmine Bromide proved that one can’t expect traditional results when performing

research. In fact through the research process the discovery of a new mechanism of binding with SrtA, which seems probabl given the endothermic data, could have been achieved. Situations in which the data one obtains is unexpected can lead to a great impact which forces the researchers to investigate and think thoroughly through the obtained data. Therefore tit is necessary for researchers to be extremely detail oriented and always searching for explanations.

When prototyping and designing to solve a problem the most probable and promising material or design does not always succeed. The first two prototypes of the front plate of the hydraulic manifold failed to be functional. The first prototype made out of HDPE was dimensioned inadequately because the screw holes did not account for the tooling diameter. This illustrated the need to think through ones design thoroughly to anticipate the possible outcomes after fabrication. Time sensitive projects can also lead to unnecessary failures when prototyping. The second HDPE prototype failed due to a lack of material which could have been easily discovered beforehand if the pressure to produce a functional prototype was handled more patiently. A valuable tool is to learn how to slow oneself in time of pressure and think critically about what will be performed in order to produce the most successful results.

Lastly, the most valuable skill of performing research of any kind is not to become discouraged by failure. Through the process of prototyping the hydraulic manifold, we experienced failure in multiple prototypes. However, through each failure, another insight as to how the design could be improved was gained. If one thinks of failure as honest feedback and works to figure out the possible aspects of the project that could have gone awry, they will have an easier time facing failure.

Engineering Standards and Realistic Constraints

Table 12. Social & Ethical Ramifications

Rule	Stakeholders	Enforcement Strategy	Elaboration
Ensure all genetic engineering of proteins are done to the appropriate standards.	-Santa Clara University	Follow the restrictions placed on the University by the NIH and FDA.	In order to isolate Sortase A, it needs to be mutated.
Ensure all testing is done appropriately.	-Design Partners -Future students working on the project -Industry representatives	Have multiple trials of the same compound with sterility preserved throughout testing.	The future testing of the successful compounds will involve clinical trials, all needing to be completed under FDA and NIH regulations.
Ensure the safety of the entire lab as our team is not the only students working in the lab.	-Design Partners -Other students in the lab	Wear protective equipment and work solely in the fume hood. Maintain Good Laboratory Practice as outlined by the NIH	Some of the compounds are extremely toxic. If precautions are not taken, the user and other students in the same lab equipment can be exposed to hazardous materials.

Table 13. Product Ramifications

Rule	Stakeholders	Enforcement Strategy	Elaboration
Ensure data is accurate.	-Design Partners -Future students working on the project -Industry Representatives	Complete all necessary controls with multiple experimental trials.	The controls ensure that the thermodynamic data obtained was derived from the interaction between the compound and the protein only.
Ensure data obtained is only shared with the appropriate individuals	-Design Partners -Professor Zhang	Share the results with team members, Professor Zhang, future team members as well as any individuals Professor Zhang has specified.	The results of this data will likely be published and sent to a biotechnology data for further testing.
Ensure submission is performed in an ethical manner	-Design Partners -Professor Zhang -Review Committees	Clearly cite all benefactors, giving credit where it is due. Go through the hurdles of submission of data appropriately	The process of submission is usually a time intensive process with multiple steps. Assistance from outside sources will most likely be required.

Bibliography

[1] “Healthcare-associated Infections (HAIs).” Centers for Disease Control and Prevention. http://www.cdc.gov/HAI/organisms/visa_vrsa/visa_vrsa.html

[2] “ABCs Report: Methicillin-Resistant *Staphylococcus Aureus* 2011”. Active Bacterial Core surveillance (ABCs). Centers for Disease Control and Prevention. http://www.cdc.gov/abcs/reports-findings/survreports/mrsa11.html

[3] “Antimicrobial Resistance” World Health Organization. May 2013. http://www.who.int/mediacentre/factsheets/fs194/en/index.html

[4] Mazmanian, Sarkis, Gwen Liu, Hung Ton-That, and Olaf Schneewind. "Staphylococcus aureus Sortase, an Enzyme that Anchors Surface Proteins to the Cell Wall." *Science Magazine*. 285.5428 (1999): 760-3. Web.

[5] Freyer, Matthew W., and Edwin A. Lewis. "Isothermal Titration Calorimetry: Experimental Design, Data Analysis, and Probing Macromolecule/Ligand Binding and Kinetic Interactions." *Methods in Cell Biology* 84 (2008): 79-113. Web.

[6] Tellinghuisen, Joel. "Isothermal Titration Calorimetry at Very Low C." *Analytical Biochemistry* 373 (2008): 395-97. Web.

[7] Carbonell, Teresa and Ernesto Freire. “Binding Thermodynamics of Statins to HMG-CoA Reductas.” *Biochemistry* 44 (2005): 11741-11748. Web.

[8] Ilangovan, Udayar, Hung Ton-That, Junji Iwahara, Olaf Schneewind, and Robert T. Clubb. "Structure of Sortase, the Transpeptidase That Anchors Proteins to the Cell Wall of Staphyloccocus Aureus." *Proceedings of the National Academy of Sciences* 98.11 (2001): 6056-6061. Web.

[9] Lu, Changsheng, and Zhiwen Zhang. "Staphylococcus Aureus Sortase A Exists as a Dimeric Protein In Vitro." *Biochemistry* 46 (2007): 9346-354. Web.

[10] Naik, Mandar T., and Robert T. Clubb. "Staphylococcus Aureus Sortase A Traspeptidase: Calcium Promotes Sorting Signal Binding By Altering the Mobility and Structure of an Active Site Loop." *The Journal of Biological Chemistry* 281.3 (2006): 1817-826. Web.

[11] Frankel, Brenda A., Matthew Bentley, Ryan G. Kruger, and Dewey G. McCafferty. "Vinyl Sulfones: Inhibitors of SrtA, a Transpeptidase Required for Cell Wall Protein

Anchoring and Virulence in Staphyloccus Aureus." *Journal of the American Chemical Society* 126 (2004): 3404-405. Web.

[12] Kim, Soo-Hwan, Dong-Sun Shin, Mi-Na Oh, Soon-Chun Chung, Jang-Suk Lee, and Ki-Bong Oh. "Inhibition of the Bacterial Surface Protein Anchoring Transpeptidase Sortase by Isoquinoline Alkaloids." *Bioscience, Biotechnology, and Biochemistry* 68.2 (2004): 421-24. Web.

[13] Kim, Soo-Whan, Il-Moo Chang, and Ki-Bong Oh. "Inhibition of the Bacterial Surface Protein Anchoring Transpeptidase Sortase by Medicinal Plants." *Bioscience, Biotechnology, and Biochemistry* 66.12 (2002): 2751-754. Web.

[14] Brown, Richard K., J. Michael Brandts, Ronan O'Brien, and William B. Peters. "ITC-derived Binding Constants." *Label-free Biosensors: Techniques and Applications*. Matthew A. Cooper. Cambridge: Cambridge UP, 2009. 223-50. Web.

Appendices

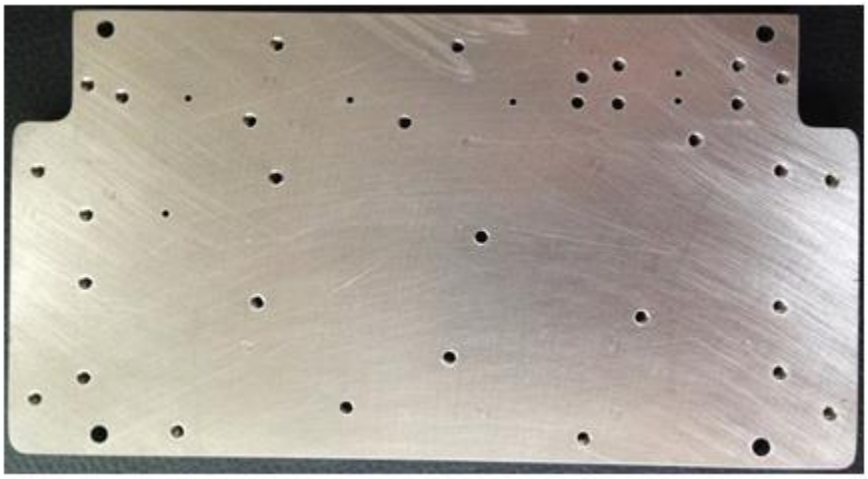

Appendix A.: Inner side of the original front plate.

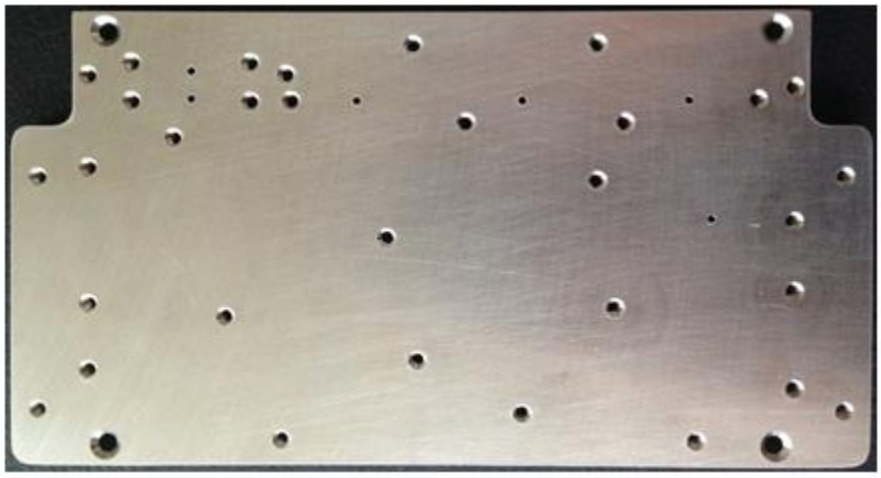

Appendix B. Outer side of the original front plate.

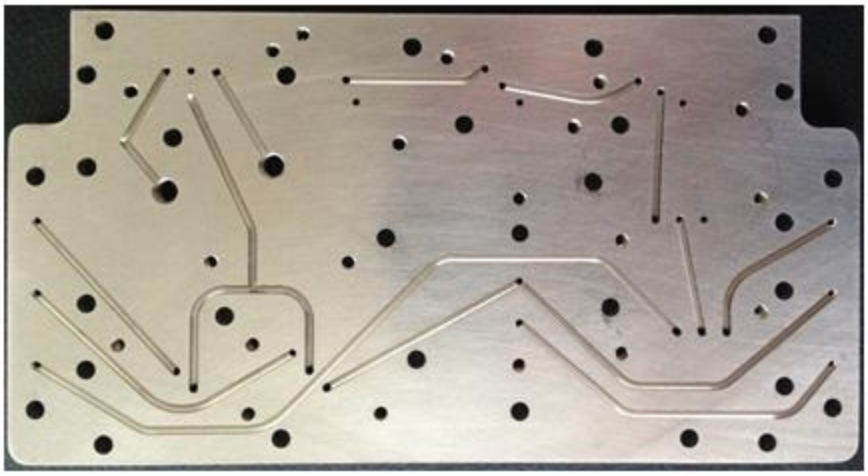

Appendix C. Inner side of the back plate which houses the microchannels to direct fluid flow.

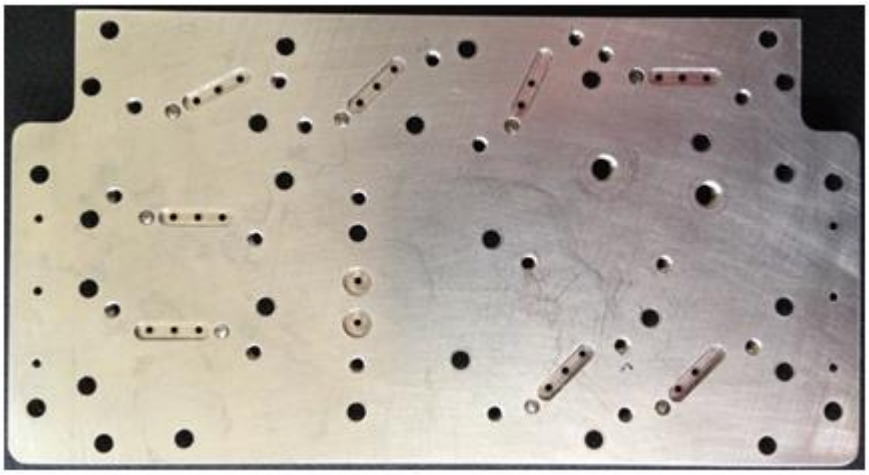

Appendix D. Outer side of the back plate which houses the solenoids, master suction pump, and structural screws.

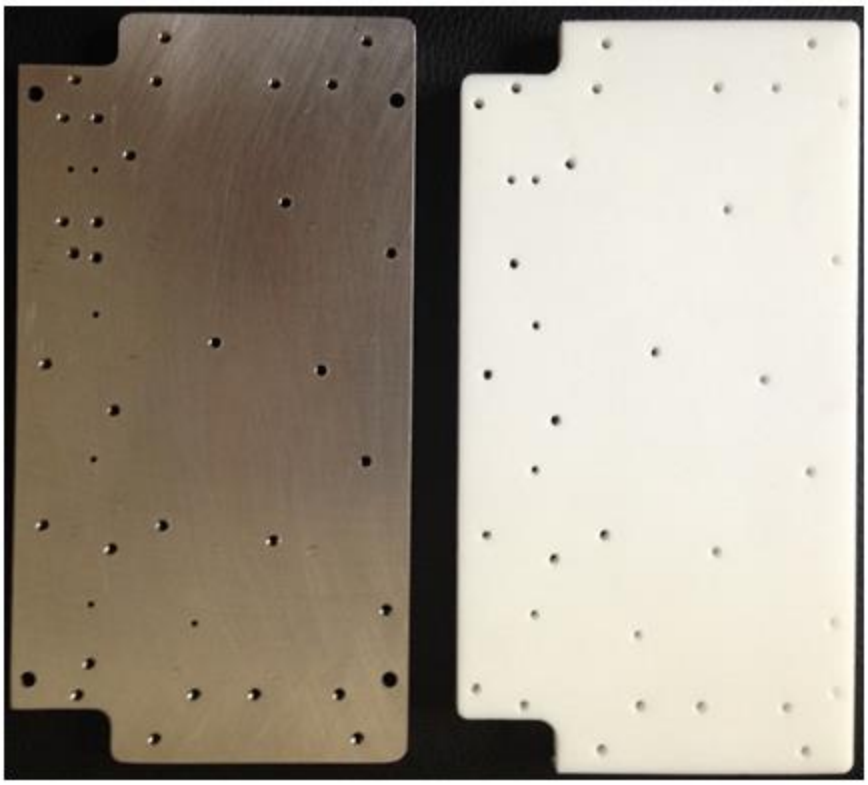

Appendix E. Side-by-side comparison of the inner side of the front plate with PTFE prototype, on the right, and the original steel front plate, on the left.

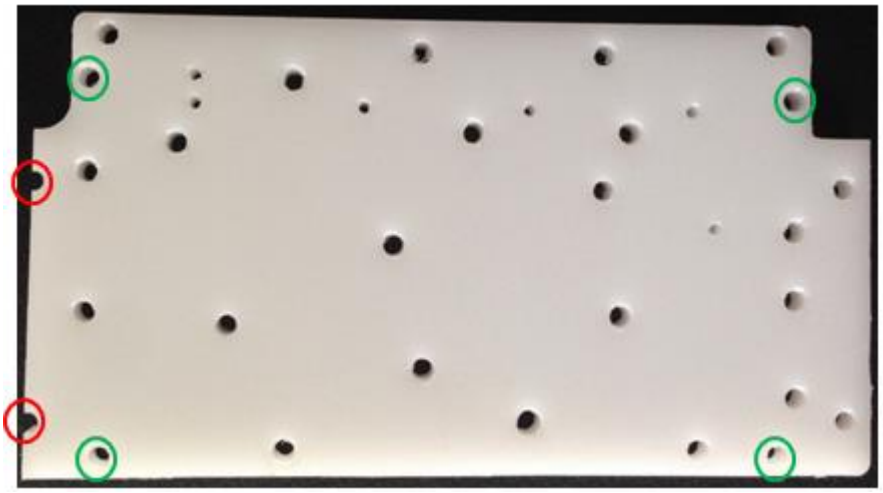

Appendix F.. Prototype 2 made out of HDPE. Contains the incomplete structural screw holes in red and the corrected structural screw holes in green. The corrected screw holes are the holes that were incomplete in Prototype 1.

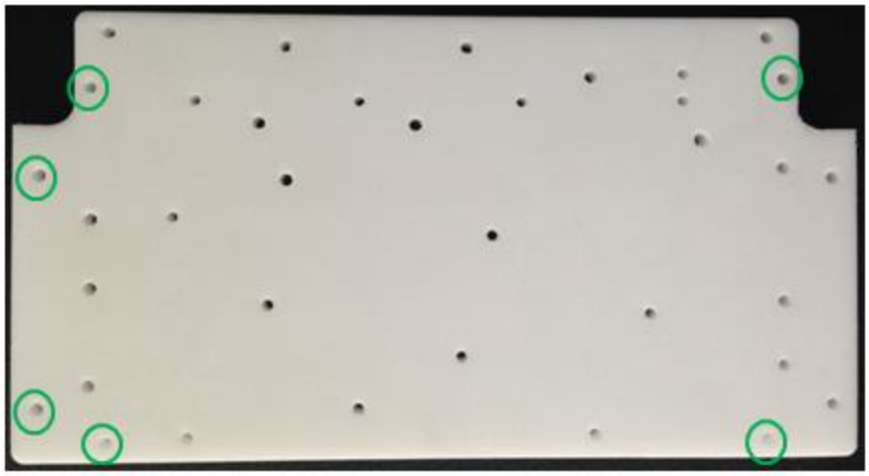

Appendix G. Prototype 3 made out of PTFE. Figure demonstrates all complete screw holes in green (those screw holes that were incomplete in prototypes 1 and 2).

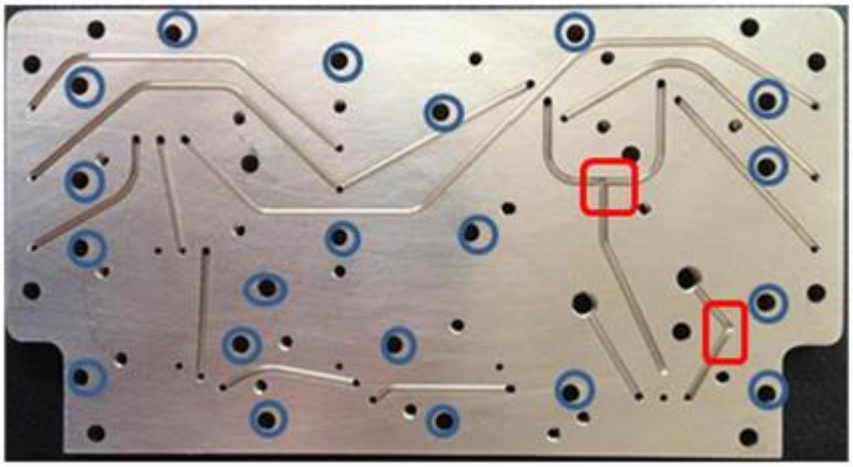

Appendix H.. Picture of the black plate of the current hydraulic manifold. The structural screws are shown in blue and examples of the hard angles of the microchannel design are in red.